

Unitary matrix integrals, symmetric polynomials, and long-range random walks

Ward L. Vleeshouwers^{1,2*} and Vladimir Gritsev¹

¹ *Institute for Theoretical Physics, Universiteit van Amsterdam,
Science Park 904, Postbus 94485, 1098 XH Amsterdam, The Netherlands*

² *Institute for Theoretical Physics, Universiteit Utrecht,
Princetonplein 5, Postbus 80.089, 3584 CC Utrecht, The Netherlands*

*w.l.vleeshouwers@uva.nl

March 9, 2023

Abstract

Unitary matrix integrals over symmetric polynomials play an important role in a wide variety of applications, including random matrix theory, gauge theory, number theory, and enumerative combinatorics. We derive novel results on such integrals and apply these and other identities to correlation functions of long-range random walks (LRRW) consisting of hard-core bosons. We generalize an identity due to Diaconis and Shahshahani which computes unitary matrix integrals over products of power sum polynomials. This allows us to derive two expressions for unitary matrix integrals over Schur polynomials, which can be directly applied to LRRW correlation functions. We then demonstrate a duality between distinct LRRW models, which we refer to as *quasi-local particle-hole duality*. We note a relation between the multiplication properties of power sum polynomials of degree n and fermionic particles hopping by n sites. This allows us to compute LRRW correlation functions in terms of auxiliary fermionic rather than hard-core bosonic systems. Inverting this reasoning leads to various results on long-range fermionic models as well. In principle, all results derived in this work can be implemented in experimental setups such as trapped ion systems, where LRRW models appear as an effective description. We further suggest specific correlation functions which may be applied to the benchmarking of such experimental setups.

Contents

1	Introduction	2
1.1	Background	2
1.2	Structure of the paper and main results	4
2	Unitary matrix integrals and Wick's theorem	7

2.1	Applying Wick's theorem	9
2.2	Generalization of an identity due to Diaconis and Shahshahani	11
2.3	Border strips and their application to unitary matrix integrals over Schur polynomials	12
2.3.1	Expansion in Schur polynomials	13
2.3.2	Expansion in power sum symmetric polynomials	18
3	Applying symmetric polynomial theory to long-range random walks	23
3.1	Elementary and complete homogeneous symmetric polynomials	23
3.1.1	Quasi-local particle-hole duality	28
3.2	Power sum symmetric polynomials and border strips	29
3.2.1	The action of the hamiltonian in terms of Young diagrams	33
3.2.2	Border strip tableaux and fermionic models	35
3.2.3	Schur polynomial expansions of correlation functions	38
3.2.4	Power sum expansions of correlation functions	39
3.2.5	Correlations for power sums and applications to experimental benchmarking	41
4	Conclusions	42
5	Acknowledgements	43
	Appendices	44
A	Symmetric polynomials and Young diagrams	44
B	Correlation functions of long-range random walks	55
C	Evaluating unitary matrix integrals	59
6	References	62

1 Introduction

1.1 Background

This work presents a study of unitary matrix integrals over symmetric polynomials and their application to correlation function of long-range random walk (LRRW) models. We derive novel results on weighted unitary integrals over symmetric polynomials. These have a wide variety of mathematical and physical applications, including to Random Matrix Ensembles (RME's) and quantum chaos, gauge theories, number theory, and enumerative combinatorics. Connections between RME's and random walks have been explored extensively, see e.g. [1], [2] for early reviews on RME's and [3], [4] for more recent ones. Random walkers are called vicious when their paths are not allowed to intersect, i.e. when there exists the restriction that no two random walkers may occupy the same site. Vicious random walk models belong to the class of random-turns models when, at each time step, we move a single random walker. On the other hand,

there are the lock-step models, where, at each time step, all random walkers are moved. For an early treatment, see [5], see also e.g. [6], [7], [8], [9], [10], [11], [12]. This work will generally consider long-range versions of the random-turns model. One way in which a relation between RME's and vicious random walks can be seen to arise is from the fact that the joint eigenvalue distribution of unitary RME's is proportional to the squared Vandermonde determinant. This leads to a vanishing probability that any two eigenvalues coincide, which is known as level repulsion in random matrix theory. In physical terms, these non-intersecting random walkers can be interpreted as fermionic or hard-core bosonic particles, see e.g. the review [13]. This leads to an interpretation of the eigenvalue probability density of models related to classical Lie groups in terms of the ground state density of non-interacting and non-intersecting particles which are subject to confining potential and certain boundary conditions. This language naturally leads to a so-called τ -functions of integrable hierarchies of differential equations with many deep results obtained over the years [14], [15], [16], [17], [18], [19]. Connection to integrability is widely used in the recent literature, see [20], [21] and also [22] for the case of unitary matrix models. Further, various correlation functions and important quantities in string theory are expressed in terms of these objects, see e.g. [23], [24] for recent developments. We also mention here applications in algebraic geometry and topology, see [4] for a review.

The connection between RME's and random walks appears in a different guise as well. Bogoliubov demonstrated [25] that the time-dependent correlation functions of the XX0-model are the generating functions of nearest neighbour vicious random walkers, i.e. those which can take only a unit size step to the left or right. Here, the XX0-model refers to the XX-model at zero magnetic field. These correlation functions can then be expressed as certain weighted unitary matrix integrals over Schur polynomials [25], [26]. In general, spin configurations which start with an infinite sequence of particles and end with an infinite sequence of holes correspond uniquely to certain Young diagrams. Time-dependent correlation functions of the XX0-model involving such configurations then take the form of unitary matrix integrals over a product of Schur polynomials associated to the corresponding Young diagrams. In the remainder of this work, we will refer to down spins as particles and up spins as holes. In the nearest neighbour case, the corresponding RME is given by the Gross-Witten-Wadia (GWW) model, where the inverse square of the coupling constant of the GWW model is proportional to the time parameter of the correlation function of the XX0-model. This relation between random walk correlation functions and matrix integrals over Schur polynomials was generalized to the case of LRRW models [27], where the particles can hop over greater distances. The particles in question behave as hard-core bosons rather than fermions, as the wave function does not acquire a minus sign when a particle hops over another one. In the long-range case, the weight function of the corresponding matrix model encodes the particular choice of LRRW model. In particular, the n^{th} hopping parameter a_n , which allows particles to hop a distance of n sites, equals the n^{th} Fourier coefficient of the weight function. The hopping parameters are required to decay as $a_n \sim n^{-1-\epsilon}$ for $\epsilon > 0$ as $n \rightarrow \infty$, corresponding to weight functions which satisfy the strong Szegő limit theorem.

The generalization to LRRW models allows for the application to long-range one-dimensional systems, such as those characterized by dipole-dipole interactions. For more recent examples of such systems, see e.g. [28]. Another physically motivated context where long-range systems are of interest is that of

Anderson localization in long-range low-dimensional hopping models [29], [30]. These systems can be simulated experimentally with trapped ions, which have been demonstrated to exhibit great tunability in terms of the range of the the relevant hopping amplitude (see e.g. [31] for a review). Further applications include the dynamics of the Loschmidt echo in 1D systems, already considered in [25], see also [32], [33]. Dynamical phase transition in Loschmidt echo has been recently observed using the matrix models tools in [34]. The Loschmidt echo, a measure of chaoticity in quantum systems [35], can be regarded as a particular realization of the τ -function mentioned above. The Loschmidt echo is also related to other important probes of many-body system dynamics, such as out-of-time-correlation functions. Importantly, the Loschmidt echo is an experimentally measurable quantity, see e.g. [36], [37], [38]. In the context of combinatorics, we mention also a relation to the plane partitions, see e.g. [33] for a recent account thereof.

In this paper, we consider physically relevant quantities, such as Loschmidt echo and various correlation functions in LRRW models, for which we employ identities on Young diagrams and the closely related theory of symmetric functions. We summarize the outline of the paper, including these results, in the remainder of the introduction.

1.2 Structure of the paper and main results

This work is structured as follows. We consider unitary matrix integrals over symmetric polynomials, which appear as correlation functions of long-range random walks of hard-core bosons. The basics of symmetric function theory, the relation between correlation functions of LRRW models and weighted unitary integrals over symmetric functions, and the evaluation of these objects are treated in appendices A, B, and C, respectively. To be precise, we consider correlation functions between configurations which begin with an infinite string of particles in the form of hard-core bosons and end with an infinite string of holes, with a finite region of mixed particles and holes in between. These correlation functions are written as follows,

$$F_{\lambda;\mu}(\tau) = \left\langle \emptyset \left| \sigma_{j_1}^+ \dots \sigma_{j_N}^+ e^{-\tau \hat{H}} \sigma_{l_1}^- \dots \sigma_{l_N}^- \right| \emptyset \right\rangle, \quad \lambda_r = j_r + r, \quad \mu_s = l_s + s, \quad (1)$$

where $|\emptyset\rangle$ is a state with holes at all lattice sites, where we remind the reader that we refer to up spins as holes and down spins as particles. The hamiltonian H is a long-range translationally-invariant hamiltonian whose hopping parameters $a_{m,n} = a_{m-n}$ decay faster than $|a_k| \sim |k|^{-1}$, see equation (225). Defining the matrix model average $\langle \dots \rangle$ for some weight function f as in (249), it was found [25], [26], [27] that this can be written (in our notation) as

$$\frac{F_{\lambda;\mu}(\tau)}{F_{\emptyset;\emptyset}(\tau)} = \langle s_\lambda(U) s_\mu(U^{-1}) \rangle, \quad (2)$$

where the dependence on the particular choice of LRRW model and the generalized time parameter τ are captured by the weight function f . Further, s_λ and s_μ are Schur polynomials, whose representations λ and μ characterize the particle-hole configurations that occupy a finite interval in between the infinite strings of particles and holes.

Sections 2 and 3 present our results, starting in 2.2 with the generalization of the result due to Diaconis and Shahshahani in [39]. Writing $p_\mu = p_{\mu_1} p_{\mu_2} \dots$, where p_n is the n^{th} power sum polynomial, our result in (36) reads

$$\langle p_\rho(U) p_\mu(U^{-1}) \rangle = \sum_{n=0}^{\tilde{n}} C_n . \quad (3)$$

where C_n and \tilde{n} are the contribution arising from performing n contractions in $\langle p_\rho p_\mu \rangle$ and the maximum number of such contractions, which are defined in (34) and (35), respectively. Essentially, this result arises from the application of Wick's theorem and the fact that $\langle p_n(U) p_k(U^{-1}) \rangle - \langle p_n(U) \rangle \langle p_k(U^{-1}) \rangle = n \delta_{n,k}$, which we derived a previous work [40]. In sections 2.3.1 and 2.3.2, we derive expansions of general correlation functions of the form $\langle s_\lambda(U) s_\nu(U^{-1}) \rangle$ in terms of Schur or power sum polynomials, respectively. Specifically, section 2.3.1 establishes a relation between correlation functions $\langle s_\lambda s_\nu \rangle$ and $\langle s_{\lambda \setminus \{\eta\}} \rangle, \langle s_{\nu \setminus \{\eta\}} \rangle^*$, where $\lambda \setminus \{\eta\}$ is a diagram obtained from λ by the removal of border strips η_j of sizes $|\eta_j| = \alpha_j$. In section 2.3.2, we express $\langle s_\lambda s_\nu \rangle$ in terms of $\langle p_\mu \rangle$, where the expansion coefficients are determined by removing border strips from λ and ν such that the resulting diagram is the same for both λ and ν . These results have a direct interpretation in terms of particle-hole configurations which is treated in section 3.2, for which reason we state these results with their particle-hole interpretations below.

We first consider the results derived in section 3.1, where we apply identities involving elementary and complete homogeneous symmetric polynomials to LRRW correlation functions. One result that arises in this way involves the well-known involution between elementary and homogeneous polynomials corresponding to the transposition of Young diagrams, which exchanges rows and columns. Although this result is mathematically trivial, its physical consequences are quite surprising and profound. Consider any two LRRW models, referred to as model A and B, whose hopping parameters are related by $a_k \rightarrow (-1)^{k+1} a_k$, and write their correlation functions as $F_{\lambda;\mu}^{(1)}(\tau)$ and $F_{\lambda;\mu}^{(2)}(\tau)$, respectively. Our result is given by equation (115), which reads

$$F_{\lambda;\mu}^{(1)}(\tau) = F_{\lambda^t;\mu^t}^{(2)}(\tau) , \quad (4)$$

where t refers to transposition of diagrams, which, combined with a parity transformation, implements a particle-hole transformation. Therefore, equation (4) states that the correlation functions of models A and B are equal after performing local particle-hole and parity transformations, which only act non-trivially on the interval in between the infinite strings of particles and holes. For this reason, we refer to this result as *Quasi-Local Particle-Hole duality* (QLPH). In this way, a basic property of symmetric polynomials leads to a surprising result on LRRW models. Further such examples, involving e.g. the Pieri formula, are given in equations (101), (102), (102), (107), (107).

Section 3.2 treats the application of identities involving power sum polynomials and border strips, including results derived in section 2.3. We find that the multiplication of power sum polynomials of degree n and the corresponding addition of border strips is related to fermionic particles hopping n sites to the right, whereas removal of such a border strip corresponds to hopping n sites to the left. This allows us to

interpret various results in terms of an auxiliary fermionic (rather than hard-core bosonic) system. This reasoning can be applied to the computation of χ_α^λ , which are the irreducible characters of the symmetric group, as we explain just above section 3.2.1. Further, combined with identities we found in [40], it leads immediately to results such as (127) and (134). In section 3.2.1, we use the relation between border strips and particle hopping to characterize the action of the hamiltonian in terms of Young diagrams.

In section 3.2.2, we use the aforementioned relation between power sums and fermions to derive two results on long-range fermionic models. First of all, from the fact that $\chi_\alpha^{\lambda/\mu}$ does not depend on the order of the entries of α leads us to conclude the following. Consider a one-dimensional fermion configuration corresponding to some diagram μ , and consider all ways of moving not necessarily distinct fermions to the right by $\alpha_1, \alpha_2, \dots$ sites, where α_j are unordered non-negative integers. We find that *the order of the step sizes α_j by which we move fermions has no effect on the outcome of this process*. That is, if we take a fermionic configuration and consecutively move fermions to the right by various step sizes, the outcome depends only on the distribution of the step sizes and not the order in which the steps are taken. Naturally, this statement also holds if we move fermions to the left instead of the right. The second result follows from the fact that $\chi_\alpha^{\lambda/\rho}$ for $\alpha = (n^k)$ is cancellation-free [41], [42]. Here, ρ is the so-called n -core of λ , which is the unique diagram that remains after removing the maximal number of size n border strips from λ . In particular, start with a particle-hole configuration, which we call λ , and consider all ways to move (not necessarily distinct) particles by n sites, where n is any finite positive integer. By taking a particle and moving it by n sites (from site j to $j+n$), it may in the process ‘jump over’ $\leq n-1$ other particles (occupying sites $j+1$ to $j+n-1$). Our result then states that all ways to go from λ to any other configuration ν involves jumping over *either* an even *or* an odd number of particles, depending only on the choice of λ and ν . When applied to a fermionic model where fermions can hop only by $\pm n$ sites for a single choice of n , this implies that there is no destructive interference between various ways to arrive at the same fermionic state, allowing for rapid spread through Hilbert space upon time evolution. The same reasoning can be applied to certain LRRW correlation functions, leading to (143) and (145).

In sections 3.2.3 and 3.2.4, we apply our results from section 2.3 to LRRW correlation functions. The expansion in 2.3.1, including its particle-hole interpretation in 3.2.3, given in (52) and (151), reads

$$\begin{aligned} \langle s_\lambda(U) s_\nu(U^{-1}) \rangle_c &= \sum_\alpha \frac{1}{z_\alpha} \left(\sum_{\{\eta\}} (-1)^{\text{ht}(T_\eta)} s_{\lambda \setminus \{\eta\}}(y) \right) \times \begin{pmatrix} y \rightarrow x \\ \lambda \rightarrow \nu \end{pmatrix} \\ &= \sum_\alpha \frac{1}{z_\alpha} \left((-1)^P s_{\lambda \setminus \{\eta\}}(y) \left\{ \begin{array}{l} \text{Distinct ways to take particles in } \lambda \\ \text{and move them } \alpha_1, \alpha_2, \dots \text{ sites to the} \\ \text{left, thereby hopping over } P \text{ particles} \end{array} \right\} \right) \times \begin{pmatrix} y \rightarrow x \\ \lambda \rightarrow \nu \end{pmatrix}. \end{aligned} \quad (5)$$

The expansion in terms of power sum polynomials derived in section 2.3.2, including its particle-hole

interpretation in 3.2.4, is given by equations (68) and (154) as

$$\begin{aligned} \langle s_\lambda(U) s_\nu(U^{-1}) \rangle &= \sum_{\omega, \gamma} \frac{p_\omega(y) p_\gamma(x)}{z_\omega z_\gamma} \sum_{\{\eta\}, \{\xi\}} (-1)^{\text{ht}(T_\eta) + \text{ht}(T_\xi)} \delta_{\lambda \setminus \{\eta\}, \nu \setminus \{\xi\}} \\ &= \sum_{\omega, \gamma} \frac{p_\omega(y) p_\gamma(x)}{z_\omega z_\gamma} (-1)^P \left\{ \begin{array}{l} \text{Distinct ways to move particles in } \lambda \text{ and } \nu \\ \text{to the left by } \gamma_1, \gamma_2, \dots \text{ and } \omega_1, \omega_2, \dots \text{ sites,} \\ \text{respectively, so hopping over } P \text{ other particles} \\ \text{and ending up in the same configuration.} \end{array} \right\}. \end{aligned} \quad (6)$$

The expansion in (6) is particularly convenient in applications where one has access to the power sum polynomials, such as for LRRW models, where they are given by $p_k = k\tau a_{\pm k}$, in terms of the hopping parameters a_k and the generalized time parameter τ . Then, in section 3.2.5 we suggest applications of some of our results to experimental benchmarking. We finish with our conclusions, as well as possible generalizations and applications of our results, which include both theoretical and experimental suggestions.

2 Unitary matrix integrals and Wick's theorem

We now proceed with the derivation of our results. In this section, we will derive expansions for unitary matrix integrals over symmetric polynomials. The reader may consult appendix C for more information on these objects. Taking the limit $N \rightarrow \infty$ allows us to apply an expression we found in [40]. For $k, n \in \mathbb{N}^+$, and $f(z) = H(x; z)H(y; z^{-1})$ satisfying the strong Szegő limit theorem, we demonstrated that

$$\langle \text{tr} U^n \text{tr} U^{-k} \rangle = n\delta_{n,k} + p_n(y)p_k(x). \quad (7)$$

For the CUE, $x_j = 0 = y_j$ for all j , so that $p_n(x) = 0$ for all n . Therefore, $\langle \text{tr} U^n \text{tr} U^{-k} \rangle_{\text{CUE}} = n\delta_{n,k}$ [43]. We briefly summarize the derivation of our more general result in (7) as we will be using similar arguments throughout the remainder of this work. We repeat that, for $n \in \mathbb{N}^+$,

$$\text{tr} U^n = p_n(e^{i\theta_j}) = \sum_{r=0}^{n-1} (-1)^r s_{(n-r, 1^r)}(U). \quad (8)$$

It is clear that this also holds when we replace U with U^{-1} . Using (259), we have

$$\langle \text{tr} U^n \rangle = p_n(y), \quad \langle \text{tr} U^{-n} \rangle = p_n(x). \quad (9)$$

Then,

$$\langle \text{tr} U^n \text{tr} U^{-k} \rangle = \sum_{\nu} \sum_{r=0}^{n-1} (-1)^r s_{(n-r, 1^r)/\nu}(y) \sum_{s=0}^{k-1} (-1)^s s_{(k-s, 1^s)/\nu}(x). \quad (10)$$

The first sum on the right hand side of runs over all representations ν satisfying $\nu \subseteq (n-r, 1^r)$ as well as $\nu \subseteq (k-s, 1^s)$. We list below the contributions arising for various choices of ν . We will often omit the

variables x and y henceforth.

1. If ν is the empty partition $\nu = \emptyset$, $s_{\lambda/\nu} = s_\lambda$ i.e. the skew Schur polynomials reduces to the usual (non-skew) Schur polynomial. This contributes

$$\sum_{r=0}^{n-1} (-1)^r s_{(n-r, 1^r)}(y) \sum_{s=0}^{k-1} (-1)^s s_{(k-s, 1^s)}(x) = p_n(y) p_k(x) . \quad (11)$$

2. If $\nu = \lambda$, the skew Schur polynomial $s_{\lambda/\nu} = s_{\lambda/\lambda} = 1$. For $\lambda = (n-r, 1^r)$ and $\mu = (k-s, 1^s)$, one can only have $\lambda = \nu = \mu$ if $k = n$ and $r = s$. For $k = n$ and $\nu = (n-r, 1^r)$ and we sum over r , we get a contribution of the following form

$$\sum_{r=0}^{n-1} (s_\emptyset)^2 = n . \quad (12)$$

This is where the term $n\delta_{n,k}$ in (7) originates.

3. Take $k \leq n$ without loss of generality. The only remaining choice for ν is $\nu \neq \emptyset$ and $\nu \neq (n-r, 1^r)$. For $\lambda = (a, 1^b)$ and $\nu = (c, 1^d)$ such that $\nu \subseteq \lambda$, we have $\lambda/\nu = (a-c) \otimes (1^{b-d})$, e.g. for $\lambda = (4, 1^2)$ and $\nu = (2, 1)$, we have the following.

$$\begin{array}{|c|c|c|c|} \hline \square & \square & \square & \square \\ \hline \square & & & \\ \hline \square & & & \\ \hline \end{array} / \begin{array}{|c|c|} \hline \square & \square \\ \hline \square & \\ \hline \end{array} = \begin{array}{|c|c|c|} \hline \square & \square & \square \\ \hline \end{array} \quad (13)$$

Fixing a single such $\nu = (a, 1^b)$ and considering only the sum over r in (10), we have

$$\sum_{r=0}^{n-1} (-1)^r s_{(n-r, 1^r)/(a, 1^b)} = \sum_{r=b}^{n-a} (-1)^r h_{n-r-a} e_{r-b} = 0 , \quad (14)$$

where we applied (162). That is, we get zero contribution for all $\nu \neq \emptyset, (n-r, 1^r)$.

Combining the above arguments leads to equation (7). Of course, the same reasoning can be applied to other expectation values involving $\text{tr}U^n$, such as

$$\langle \text{tr}U^{-n} s_\lambda(U) \rangle_c = \sum_{\nu \neq \emptyset} \sum_{r=0}^{n-1} (-1)^r s_{(n-r, 1^r)/\nu} s_{\lambda/\nu} . \quad (15)$$

As mentioned in appendix C, the connected expectation value $\langle \dots \rangle_c$ in the above equation is given by $\langle AB \rangle_c = \langle AB \rangle - \langle A \rangle \langle B \rangle$. The sum in (15) is over all $\nu \neq \emptyset$ such that $\nu \subseteq \lambda, (n-r, 1^r)$. Fixing any $\nu \subseteq (n-r, 1^r)$ in (15) with $\nu \neq (n-r, 1^r)$ gives zero when summing over r by application of (14). Therefore, we only get a non-zero answer for terms for which $\nu = (n-1, 1^r) \subseteq \lambda$. That is,

$$\langle \text{tr}U^{-n} s_\lambda(U) \rangle_c = \sum_r (-1)^r s_{\lambda/(n-1, 1^r)} , \quad (16)$$

where the sum is over $\min(0, n - \lambda_1) \leq r \leq \min(n - 1, \lambda_1^t + 1)$. Using (197), we can express this as

$$\langle \text{tr} U^{-n} s_\lambda(U) \rangle_c = \sum_{\nu} (-1)^{\text{ht}(\lambda/\nu)} s_{\nu} , \quad (17)$$

where the sum is over all ν such that λ/ν is a border strip η of size n , which we also write as $\nu = \lambda \setminus \eta$. More information on border strips can be found in appendix A, see equation (179) and especially (201) and below. As an example, take $\lambda = (6, 4, 3^2, 2)$ and $n = 4$. We show the diagrams ν appearing in (17) below, where the cells that are removed are again given in black.

$$- \begin{array}{|c|c|c|c|c|c|} \hline & & & \blacksquare & \blacksquare & \blacksquare \\ \hline & & & \blacksquare & & \\ \hline & & & & & \\ \hline & & & & & \\ \hline & & & & & \\ \hline & & & & & \\ \hline \end{array} + \begin{array}{|c|c|c|c|c|c|} \hline & & & & & \\ \hline & & \blacksquare & \blacksquare & \blacksquare & \\ \hline & & \blacksquare & & & \\ \hline & & \blacksquare & & & \\ \hline & & & & & \\ \hline & & & & & \\ \hline \end{array} - \begin{array}{|c|c|c|c|c|c|} \hline & & & & & \\ \hline & & & & & \\ \hline & & & & & \\ \hline & & \blacksquare & \blacksquare & & \\ \hline & & \blacksquare & & & \\ \hline & & & & & \\ \hline \end{array} \quad (18)$$

2.1 Applying Wick's theorem

We will now combine equation (7) with Wick's theorem to compute more complicated objects. In particular, for terms of the form $\langle \text{tr} U^{n_1} \text{tr} U^{n_2} \dots \text{tr} U^{-k_1} \text{tr} U^{-k_2} \dots \rangle$, we sum over all ways to contract between copies of $\text{tr} U^{n_j}$ and $\text{tr} U^{k_m}$. This contraction is done using the connected version of equation (7), which equals the CUE result,

$$\langle \text{tr} U^n \text{tr} U^{-k} \rangle_c = n \delta_{n,k} . \quad (19)$$

We first consider how Wick's theorem arises from the properties of Young diagrams for some relatively simple cases. For example, we have

$$\langle (\text{tr} U^2)^2 \text{tr} U^{-1} \rangle_c = 2 \langle \text{tr} U \text{tr} U^{-2} \rangle_c \langle \text{tr} U^{-2} \rangle_c = 0 , \quad (20)$$

where the factor two in the second expression arises from the fact that there are two ways to contract between $(\text{tr} U^2)^2$ and $\text{tr} U^{-1}$, which both contribute a term proportional to $\langle \text{tr} U \text{tr} U^{-2} \rangle_c = 0$. We will now express the same equation using Young diagrams. Using (175), the diagrams corresponding to $\text{tr} U^2$ are as follows:

$$\begin{array}{|c|c|} \hline & \\ \hline & \\ \hline \end{array} - \begin{array}{|c|} \hline \\ \hline \\ \hline \end{array} \quad (21)$$

We take the square of the above expression and apply equation (195) (or, in this case, the Pieri formulas (186) and (187)) to find the diagrams contributing to $(\text{tr} U^2)^2$. These are as follows.

$$\begin{array}{ccccccc}
\boxed{} & \boxed{} & \boxed{} & \boxed{} & - & \begin{array}{ccc} \boxed{} & \boxed{} & \boxed{} \\ \boxed{} & & \end{array} & + & 2 & \begin{array}{cc} \boxed{} & \boxed{} \\ \boxed{} & \boxed{} \end{array} & - & \begin{array}{cc} \boxed{} & \boxed{} \\ \boxed{} & \\ \boxed{} & \end{array} & + & \begin{array}{c} \boxed{} \\ \boxed{} \\ \boxed{} \\ \boxed{} \end{array}
\end{array} \tag{22}$$

We will denote the above sum over diagrams as $\sum_{\lambda} b_{\lambda} s_{\lambda}$, i.e. $b_{(4)} = 1$, $b_{(3,1)} = -1$, $b_{(2,2)} = 2$, $b_{(2,1,1)} = -1$, $b_{(1^4)} = 1$. Applying (257), we have

$$\langle (\text{tr} U^2)^2 \text{tr} U^{-1} \rangle_c = \sum_{\lambda} b_{\lambda} s_{\lambda/\square} \tag{23}$$

That is, we take $\sum_{\lambda} b_{\lambda} s_{\lambda}$ and find the skew diagrams λ/\square , found by removing a single cell from λ which has no cells to its right or below it. From these constraints, it follows that the resulting object after removing a cell is still a valid, non-skew diagram. This gives the following sum over diagrams, which evidently mutually cancel.

$$\begin{array}{ccccccc}
\begin{array}{cccc} \boxed{} & \boxed{} & \boxed{} & \blacksquare \end{array} & - & \begin{array}{ccc} \boxed{} & \boxed{} & \boxed{} \\ \blacksquare & & \end{array} & - & \begin{array}{ccc} \boxed{} & \boxed{} & \blacksquare \\ \boxed{} & & \end{array} & + & 2 & \begin{array}{cc} \boxed{} & \boxed{} \\ \boxed{} & \blacksquare \end{array} \\
- & \begin{array}{ccc} \boxed{} & \boxed{} & \\ \boxed{} & \blacksquare & \end{array} & - & \begin{array}{ccc} \boxed{} & \blacksquare & \\ \boxed{} & & \\ \boxed{} & & \end{array} & + & \begin{array}{c} \boxed{} \\ \boxed{} \\ \boxed{} \\ \blacksquare \end{array} & = & 0
\end{array} \tag{24}$$

We thus explicitly confirm that Wick's theorem is satisfied for the case of equation (20). Consider now $\langle (\text{tr} U^2)^2 \text{tr} U^{-2} \rangle_c$. Using (7), this should give

$$\langle (\text{tr} U^2)^2 \text{tr} U^{-2} \rangle_c = 2 \langle \text{tr} U^2 \text{tr} U^{-2} \rangle_c \langle \text{tr} U^2 \rangle = 4 \langle \text{tr} U^2 \rangle \tag{25}$$

We will check this explicitly as well. Applying (17) to $\sum_{\lambda} b_{\lambda} s_{\lambda}$ gives

$$\langle (\text{tr} U^2)^2 \text{tr} U^{-2} \rangle_c = \sum_{\lambda} b_{\lambda} [s_{\lambda/(2)} - s_{\lambda/(1^2)}] = \sum_{\lambda} b_{\lambda} \sum_{\nu} (-1)^{\text{ht}(\lambda/\nu)} s_{\nu}, \tag{26}$$

where the sum is over all ν such that λ/ν is a border strip of size 2, i.e. $\lambda/\nu = \begin{array}{cc} \boxed{} & \boxed{} \end{array}$ or $\lambda/\nu = \begin{array}{c} \boxed{} \\ \boxed{} \end{array}$. In terms of diagrams, this is given below. The first three diagrams corresponds to $\lambda/\nu = \begin{array}{cc} \boxed{} & \boxed{} \end{array}$ whereas the latter three correspond to $\lambda/\nu = \begin{array}{c} \boxed{} \\ \boxed{} \end{array}$, which appear with a minus sign due to the factor $(-1)^{\text{ht}(\lambda/\nu)}$.

$$\begin{array}{ccccccccccc}
\begin{array}{ccc} \boxed{} & \boxed{} & \blacksquare \end{array} & - & \begin{array}{cc} \boxed{} & \blacksquare \\ \boxed{} & \end{array} & + & 2 & \begin{array}{cc} \boxed{} & \boxed{} \\ \blacksquare & \end{array} & - & 2 & \begin{array}{cc} \boxed{} & \blacksquare \\ \boxed{} & \end{array} & + & \begin{array}{cc} \boxed{} & \boxed{} \\ \blacksquare & \end{array} & - & \begin{array}{c} \boxed{} \\ \blacksquare \\ \boxed{} \\ \blacksquare \end{array} & = & 4 & \begin{array}{cc} \boxed{} & \boxed{} \end{array} & - & 4 & \begin{array}{c} \boxed{} \\ \boxed{} \end{array}
\end{array} \tag{27}$$

We see that $\langle (\text{tr}U^2)^2 \text{tr}U^{-2} \rangle_c = 2 \langle \text{tr}U^2 \text{tr}U^{-2} \rangle_c \langle \text{tr}U^2 \rangle = 4 \begin{array}{|c|c|} \hline \square & \square \\ \hline \end{array} - 4 \begin{array}{|c|} \hline \square \\ \hline \end{array} = 4 \langle \text{tr}U^2 \rangle$, thus confirming (25). Lastly, we will briefly check

$$\langle (\text{tr}U^2)^2 (\text{tr}U^{-1})^2 \rangle_c = 0. \quad (28)$$

We have

$$\begin{array}{|c|} \hline \square \\ \hline \end{array} \otimes \begin{array}{|c|} \hline \square \\ \hline \end{array} = \begin{array}{|c|c|} \hline \square & \square \\ \hline \end{array} + \begin{array}{|c|} \hline \square \\ \hline \square \\ \hline \end{array} \quad (29)$$

Note that $\begin{array}{|c|} \hline \square \\ \hline \end{array}$ appears with a positive sign, instead of with a minus sign as it does for $\text{tr}U^2$. Then,

$$\langle (\text{tr}U^2)^2 (\text{tr}U^{-1})^2 \rangle_c = s_{\square} \sum_{\lambda} b_{\lambda} s_{\lambda/\square} \overset{0}{\cancel{\lambda}} + \sum_{\lambda} b_{\lambda} [s_{\lambda/(2)} + s_{\lambda/(1^2)}], \quad (30)$$

where we applied the fact that $\sum_{\lambda} b_{\lambda} s_{\lambda/\square} = 0$, see the diagrams in equation (24). Note that (30) gives an equation very similar to (26), but now $s_{\lambda/(1^2)}$ carries a positive sign. This gives the same six diagrams as in the top line of equation (27), except that the last three diagrams are multiplied by -1 , as can be seen below.

$$\begin{array}{|c|c|} \hline \square & \square \\ \hline \end{array} - \begin{array}{|c|} \hline \square \\ \hline \square \\ \hline \end{array} + 2 \begin{array}{|c|c|} \hline \square & \square \\ \hline \end{array} + 2 \begin{array}{|c|} \hline \square \\ \hline \square \\ \hline \end{array} - \begin{array}{|c|c|} \hline \square & \square \\ \hline \end{array} + \begin{array}{|c|} \hline \square \\ \hline \square \\ \hline \end{array} = 0 \quad (31)$$

This confirms equation (28). From these relatively simple examples, one can explicitly see how Wick's theorem arises from equation (257) and the multiplication rules for Young diagrams given in appendix A. We proceed to apply Wick's theorem to the computation of more general objects in the remainder of this section.

2.2 Generalization of an identity due to Diaconis and Shahshahani

We use Wick's theorem and equation (7) to generalize an identity due to Diaconis and Shahshahani [39], see also [43]. Writing $p_{\rho} = p_{\rho_1} p_{\rho_2} \dots p_{\rho_{\ell(\rho)}}$ and $m_j(\rho) = \text{Card}\{k : \rho_k = j\}$, as in equations (164) and (165), respectively, we wish to calculate $\langle p_{\rho}(U) p_{\mu}(U^{-1}) \rangle$. This is written out as follows,

$$\langle p_{\rho}(U) p_{\mu}(U^{-1}) \rangle = \left\langle (\text{tr}U^{j_1})^{m_{j_1}(\rho)} (\text{tr}U^{j_2})^{m_{j_2}(\rho)} \dots (\text{tr}U^{-k_1})^{m_{k_1}(\mu)} (\text{tr}U^{-k_2})^{m_{k_2}(\mu)} \dots \right\rangle. \quad (32)$$

We start with a simpler object that we can easily apply Wick's theorem to. We see that performing n contractions on $\langle (\text{tr}U^j)^a (\text{tr}U^{-j})^b \rangle$ leads to the following expression

$$C_{n,j} := \frac{a!b!j^n}{(a-n)!(b-n)!n!} p_j(x)^{b-n} p_j(y)^{a-n}, \quad n \leq \text{Min}(a, b). \quad (33)$$

Further, we have $C_{n,j} = 0$ for $n \geq \text{Min}(a, b) + 1$. Equation (33) arises as follows. There are $\frac{a!b!}{(a-n)!(b-n)!n!}$ ways to perform n contractions between $(\text{tr}U^j)^a$ and $(\text{tr}U^{-j})^b$, and the contracted terms give a contribution equal to $(\langle \text{tr}U^j \text{tr}U^{-j} \rangle_c)^n = j^n$. The $a + b - 2n$ uncontracted traces contribute $\langle \text{tr}U^j \rangle^{a-n} \langle \text{tr}U^{-j} \rangle^{b-n} = p_j(x)^{b-n} p_j(y)^{a-n}$. We now consider all possible ways to perform n contractions between $p_\rho(U)$ and $p_\mu(U^{-1})$. This leads to a sum over $\alpha = (\alpha_1, \alpha_2, \dots)$ which are partitions of n , which specify the contractions that are performed. In particular, $m_j(\alpha)$ gives the number of $\text{tr}U^j$ and $\text{tr}U^{-j}$ which are contracted. The contribution coming from n contractions in $\langle p_\rho(U)p_\mu(U)^{-1} \rangle$ can then be written as

$$C_n = \sum_{\alpha} \prod_j C_{m_j(\alpha), j}, \quad (34)$$

where the sum is over α that are partitions of n . We denote by \tilde{n} is the maximal number of contractions one can perform, which is given by

$$\tilde{n} = \text{Max}(n) = \sum_{j \geq 1} \text{Min}(m_j(\rho), m_j(\mu)). \quad (35)$$

Summing over all possible contractions and applying (33) and (34), we arrive at our result

$$\boxed{\langle p_\rho(U)p_\mu(U^{-1}) \rangle = \sum_{n=0}^{\tilde{n}} C_n.} \quad (36)$$

As mentioned before, this is a generalization of a result in [39], which considered the CUE, where $f = 1$ so that $p_j(x) = 0$ for all $j \neq 0$. Therefore, in the CUE case, one only gets a non-zero result when $\rho = \mu$. In our notation, their result reads

$$\langle p_\rho(U)p_\mu(U^{-1}) \rangle_{\text{CUE}} = z_\rho \delta_{\rho, \mu}, \quad (37)$$

where $\delta_{\rho, \mu} = 1$ for $\rho = \mu$ and zero otherwise. Note that (37) is only the last term in the full expansion in (36), corresponding to $n = \tilde{n} = \sum_j m_j(\rho)$, so that all power sums in $p_\rho(U)$ and $p_\mu(U^{-1})$ are contracted.

2.3 Border strips and their application to unitary matrix integrals over Schur polynomials

We will derive two expressions for general $\langle s_\lambda(U)s_\nu(U^{-1}) \rangle$ which rely on removing border strips from λ and ν . The first of these, equation (52), relates $\langle s_\lambda(U)s_\nu(U^{-1}) \rangle$ to sums over $\langle s_\mu(U) \rangle \langle s_\rho(U^{-1}) \rangle = s_\mu(y)s_\rho(x)$, where μ and ρ are related to λ and ν by the removal of border strips, respectively. The second expression, in equation (68), provides an expansion of $\langle s_\lambda(U)s_\nu(U^{-1}) \rangle$ in terms of the power sums $p_k(x)$ and $p_k(y)$. The latter expression appears to be particularly useful, as power sums are simpler objects than general Schur polynomials. In the context of LRRW models, $p_k(x)$ and $p_k(y)$ are given by $\pm \tau k a_{\pm k}$, where $a_{\pm k}$ are the hopping parameters in (225). Equation (68) therefore provides an expansion in τ , where the expansion coefficients depend on a_k which can be read off from the hamiltonian. We will treat the application of

these formulas to LRRW models in sections 3.2.3 and 3.2.4.

2.3.1 Expansion in Schur polynomials

From (197), (201), and (17), we have

$$\langle s_\lambda p_n \rangle_c = \sum_{\eta} (-1)^{\text{ht}(\eta)} \langle s_{\lambda \setminus \eta} \rangle = \sum_{\mu} \frac{\chi_{\mu}^{\lambda}}{z_{\mu}} \langle p_{\mu - (n)} \rangle n m_n(\mu) , \quad (38)$$

where the sum is over all μ containing a row of size n and $\mu - (n)$ is the remainder of μ after removing a row of size n . We remind the reader that $\lambda \setminus \eta$ is the diagram that results from λ after removing border strip η with (in this case) $|\eta| = n$. We can also use the recursive definition of χ_{μ}^{λ} in equation (208) to see that the second equality in (38) should hold. From (165), it is clear that

$$z_{\mu} = z_{\mu - (n)} n m_n(\mu) . \quad (39)$$

Plugging this into the rightmost expression in (38) and applying (208) leads to

$$\langle s_\lambda p_n \rangle_c = \sum_{\mu} \sum_{\eta} (-1)^{\text{ht}(\eta)} \frac{\chi_{\mu - (n)}^{\lambda \setminus \eta}}{z_{\mu - (n)}} \langle p_{\mu - (n)} \rangle . \quad (40)$$

We can then apply equation (201), which leads to the second equality in (38). If we insert two identical power sums, we find the following

$$\begin{aligned} \langle s_\lambda p_n^2 \rangle_c &= \sum_{\eta, \zeta} (-1)^{\text{ht}(\eta) + \text{ht}(\zeta)} \langle s_{(\lambda \setminus \eta) \setminus \zeta} \rangle + 2 \langle p_n \rangle \langle s_\lambda p_n \rangle_c \\ &= \sum_{\mu} \frac{\chi_{\mu}^{\lambda}}{z_{\mu}} \langle p_{\mu - (n^2)} \rangle 2n^2 m_n(\mu) (m_n(\mu) - 1) + 2 \langle p_n \rangle \langle s_\lambda p_n \rangle_c , \end{aligned} \quad (41)$$

where we consecutively remove border strips η and ζ satisfying $|\eta| = n = |\zeta|$, resulting in the partition $(\lambda \setminus \eta) \setminus \zeta$. The sum on the right hand side runs over all μ containing (at least) two rows of length n , and $\mu - (n^2)$ is the remainder of μ after removing two such rows. The term $2 \langle p_n \rangle \langle s_\lambda p_n \rangle_c$ arises from a single contraction between p_n and s_λ . We can again apply equation (208) to demonstrate the second equality in (41), where we focus on the term arising from two contractions. Plugging

$$z_{\mu} = z_{\mu - (n^2)} n^2 m_n(\mu) (m_n(\mu) - 1) . \quad (42)$$

into the first term on the right of (41) leads to

$$\sum_{\mu} \sum_{\zeta, \eta} (-1)^{\text{ht}(\zeta) + \text{ht}(\eta)} \frac{\chi_{\mu - (n^2)}^{(\lambda \setminus \eta) \setminus \zeta}}{z_{\mu - (n^2)}} \langle p_{\mu - (n^2)} \rangle , \quad (43)$$

which, by (201), recovers the top line of (41).

We then take $\langle s_\lambda(p_n)^k \rangle$ and perform all k contractions. This gives an object we denote by $C(n, k; \lambda)$, which equals

$$C(n, k; \lambda) = \sum_{\mu} \frac{\chi_{\mu}^{\lambda}}{z_{\mu}} \langle p_{\mu-(n^k)} \rangle k! n^k \frac{m_n(\mu)!}{(m_n(\mu) - k)!} = \sum_{\{\eta\}} (-1)^{\text{ht}(T_{\eta})} \langle s_{\lambda \setminus \{\eta\}} \rangle . \quad (44)$$

The sum on the left is over all μ containing at least k rows of length n . The sum on the right is over k border strips $\{\eta\} = \{\eta_1, \dots, \eta_k\}$ satisfying $|\eta_j| = n$ for all j , where $\lambda \setminus \{\eta\}$ is the diagram obtained after removing all η_j from λ , and T_{η} is the BST consisting of the union of η_1, \dots, η_k . It follows that the term in (44) gives zero if it is not possible to construct a subdiagram of λ with k border strips of size n , e.g. simply if $|\lambda| < nk$. Note that $C(n, 1; \lambda) = \langle s_{\lambda} p_n \rangle_c$ and $C(n, 2; \lambda) = \langle s_{\lambda} p_n^2 \rangle_c - 2 \langle p_n \rangle \langle s_{\lambda} p_n \rangle_c$.

We now consider

$$\langle s_{\lambda}(U) s_{\nu}(U^{-1}) \rangle_c = \sum_{\mu, \rho} \frac{\chi_{\mu}^{\lambda}}{z_{\mu}} \frac{\chi_{\rho}^{\nu}}{z_{\rho}} \langle p_{\mu}(U) p_{\rho}(U^{-1}) \rangle . \quad (45)$$

When we consider those μ and ρ that contain a row of size n and we contract a single copy of p_n between $p_{\mu}(U)$ and $p_{\rho}(U^{-1})$, we get an object we denote by $A(n, 1; \lambda, \nu)$, which is given by

$$A(n, 1; \lambda, \nu) = \sum_{\mu, \rho} \frac{\chi_{\mu}^{\lambda}}{z_{\mu}} \frac{\chi_{\rho}^{\nu}}{z_{\rho}} n m_n(\mu) m_n(\rho) \langle p_{\mu-(n)}(U) \rangle \langle p_{\rho-(n)}(U^{-1}) \rangle = \frac{1}{n} \langle s_{\lambda} p_n \rangle_c \langle s_{\nu} p_n \rangle_c . \quad (46)$$

Using (38) gives

$$A(n, 1; \lambda, \nu) = \frac{1}{n} C(n, 1; \lambda) C(n, 1; \nu) = \frac{1}{n} \left(\sum_{\eta} (-1)^{\text{ht}(\eta)} \langle s_{\lambda \setminus \eta} \rangle \right) \left(\sum_{\zeta} (-1)^{\text{ht}(\zeta)} \langle s_{\nu \setminus \zeta} \rangle \right) , \quad (47)$$

where the sums are again over border strips satisfying $|\eta| = n = |\zeta|$. Consider now μ and ρ that contain at least two rows of length n and contract two copies of p_n between $p_{\mu}(U)$ and $p_{\rho}(U^{-1})$,

$$\begin{aligned} A(n, 2; \lambda, \nu) &= \sum_{\mu, \rho} \frac{\chi_{\mu}^{\lambda}}{z_{\mu}} \frac{\chi_{\rho}^{\nu}}{z_{\rho}} \frac{n^2}{2} m_n(\mu) (m_n(\mu) - 1) m_n(\rho) (m_n(\rho) - 1) \langle p_{\mu-(n)}(U) \rangle \langle p_{\rho-(n)}(U^{-1}) \rangle \\ &= \frac{1}{2n^2} C(n, 2; \lambda) C(n, 2; \nu) . \end{aligned} \quad (48)$$

More generally, performing k contractions between $(\text{tr} U^n)^k$ and $(\text{tr} U^{-n})^k$ results in

$$A(n, k; \lambda, \nu) = \frac{1}{k! n^k} C(n, k; \lambda) C(n, k; \nu) . \quad (49)$$

Consider a partition α and, as above, contract over α_1 copies of $p_1(U)$ and $p_1(U^{-1})$, α_2 copies of $p_2(U)$ and $p_2(U^{-1})$, etc. This gives the following.

$$A(n, \alpha; \lambda, \nu) = \frac{1}{z_{\alpha}} \prod_{j \geq 1} C(n, \alpha_j; \lambda) C(n, \alpha_j; \nu) . \quad (50)$$

We can apply the above expression and (44), leading to

$$\langle s_\lambda s_\nu \rangle_c = \sum_\alpha \frac{1}{z_\alpha} \prod_{j \geq 1} C(n, \alpha_j; \lambda) C(n, \alpha_j; \nu) , \quad (51)$$

which can be written out as

$$\langle s_\lambda(U) s_\nu(U^{-1}) \rangle_c = \sum_\alpha \frac{1}{z_\alpha} \left(\sum_{\{\eta\}} (-1)^{\text{ht}(T_\eta)} s_{\lambda \setminus \{\eta\}}(y) \right) \times \begin{pmatrix} y \rightarrow x \\ \lambda \rightarrow \nu \end{pmatrix} . \quad (52)$$

The second sum above is over all border strips η_j satisfying $|\eta_j| = \alpha_j$. The above equation can be interpreted as follows. For any α , consider all ways to remove α_1 border strips of unit size (single cells) from λ and ν , α_2 border strips of size 2, α_3 of size 3, and so on. The resulting diagrams are written as $\lambda \setminus \{\eta\}$ and idem for $\lambda \rightarrow \nu$. Remember from equation (208) and the comments below that the resulting diagrams do not depend on the order of the entries of α , that is, on the order in which we remove border strips of various sizes. Indeed, the diagrams resulting from this procedure only depend on λ and the set of cardinalities $m_j(\alpha) = \text{Card}\{k : \lambda_k = j\}$.

Equation (52) expresses general expectation values $\langle s_\lambda s_\nu \rangle_c$ in terms of the non-skew Schur polynomials corresponding to $\lambda \setminus \{\eta\}$ and $\nu \setminus \{\eta\}$. On the other hand, equation (257), which is our starting point, gives an expansion in terms of skew Schur polynomials. There are various applications where an expression in terms of non-skew Schur polynomials is desirable. In general, this may be due to the fact that there are many more skew diagrams than non-skew ones, so that an expansion in non-skew diagrams may reveal underlying structures that are otherwise difficult to discern. This is also the case for the LRRW correlation functions we will be considering in the next section, where equation (52) will reveal relations between various correlation functions.

We consider now the special case where one can form BST's of shapes λ and ν from α_j border strips of size j , summed over j , such that we can fully contract between $p_\mu(U)$ and $p_\rho(U^{-1})$. That is, we consider the case where we can completely tile both λ and ν with α_1 single cells, α_2 border strips of size 2 (dominoes), and so on, for the same choice of α . This clearly requires $|\lambda| = |\nu| = \sum_{j \geq 1} j \alpha_j$, which is a necessary (but far from sufficient) condition for $\chi_\alpha^\lambda, \chi_\alpha^\nu \neq 0$. Consider the CUE, where $\langle s_{\lambda/\mu}(U^{\pm 1}) \rangle = 0$ for any $\lambda/\mu \neq \emptyset$. Applying the Murnaghan-Nakayama formula given in equation (206),

$$\sum_{\alpha_1, \dots, \alpha_k} (-1)^{\text{ht}(T_\alpha)} = \chi_\alpha^\lambda , \quad (53)$$

we then find that

$$\langle s_\lambda s_\nu \rangle_{\text{CUE}} = \sum_\alpha z_\alpha^{-1} \chi_\alpha^\lambda \chi_\alpha^\nu = \delta_{\lambda, \nu} . \quad (54)$$

This is just the orthonormality property of symmetric group characters, see e.g. [Proposition 7.17.6b, [44]].

Another way to arrive at the same expression is to directly plug equation (37),

$$\langle p_\mu p_\rho \rangle_{\text{CUE}} = z_\mu \delta_{\mu,\rho} , \quad (55)$$

into equation (45) to find the orthonormality relation in (54).

We work out the explicit example for $\lambda = (3, 2)$, which is a sufficiently small partition that we can still apply (257) for comparison. Indeed, applying (257) to $\langle s_{(3,2)} s_{(3,2)} \rangle_c = \sum_\nu s_{(3,2)/\nu} s_{(3,2)/\nu}$ gives the following diagrams $(3, 2)/\nu$.

$$\begin{array}{c} \square \square \square \\ \square \square \end{array} , \quad \begin{array}{c} \square \square \\ \square \end{array} , \quad \square \square \square , \quad \square \square , \quad \square \square , \quad 2 \square , \quad \emptyset \quad (56)$$

Note that \square appears with multiplicity 2 as it arises from $\nu = (3, 1)$ and $\nu = (2^2)$. By applying (197) for $n = 1$ (or, equivalently, (188) or (189)) to the leftmost diagram, we find the following.

$$\begin{array}{c} \square \square \square \\ \square \square \end{array} = \begin{array}{c} \square \square \\ \square \square \end{array} + \begin{array}{c} \square \square \square \\ \square \end{array} \quad (57)$$

This leads to

$$\langle s_{(3,2)} s_{(3,2)} \rangle_c = (s_{(2,2)} + s_{(3,1)})^2 + (s_{(3)} + s_{(2,1)})^2 + s_{(2,1)}^2 + (s_{(2)} + s_{(1^2)})^2 + s_{(2)}^2 + 2s_{(1)}^2 + 1 . \quad (58)$$

Note that the above equation is strictly speaking only correct when $x = y$. For $x \neq y$, we have e.g. $(s_{(2,2)}(x) + s_{(3,1)}(x))(s_{(2,2)}(y) + s_{(3,1)}(y))$ instead of $(s_{(2,2)} + s_{(3,1)})^2$, but we write it as above to avoid clutter.

We now apply (52) to compute $\langle s_{(3,2)} s_{(3,2)} \rangle_c$. To do so, we successively remove border strips from $(3, 2)$ to find the various partitions $(3, 2) \setminus \{\eta\}$ in (52). This is illustrated below, where two diagrams connected by an arrow as $\xrightarrow{p_j}$ again indicates that partitions λ and μ are related by the removal of a border strip of size j . The graph below contains all information about the removal of border strips from $(3, 2)$, except for those cases where the removal of a border strip leads to the empty diagram. All diagrams in figure 1 except for $(3, 2)$ and $(2, 2)$ are hook shapes and therefore border strips, so that they are related to \emptyset by the removal of a single border strip.

The number of ways to arrive at a diagram by following the arrows in figure 1 gives the multiplicity of that diagram in (52). For example, for $\begin{array}{c} \square \square \square \\ \square \square \end{array}$, the diagram \square has multiplicity 5 for $\alpha = (1^5)$, as there are 5 distinct ways to arrive at \square following arrows indicated by p_1 in figure 1. For α containing elements of different sizes, a single ordering should be fixed to find the correct multiplicity i.e. we do not sum over different compositions of the same cycle type. Applying equation (52) then leads to (59), where we indicate the compositions α of the power sum p_α over which we contract. That is, to arrive at a term indicated by some α , one should start from $\begin{array}{c} \square \square \square \\ \square \square \end{array}$ and follow arrows indicated by the α_j in any order,

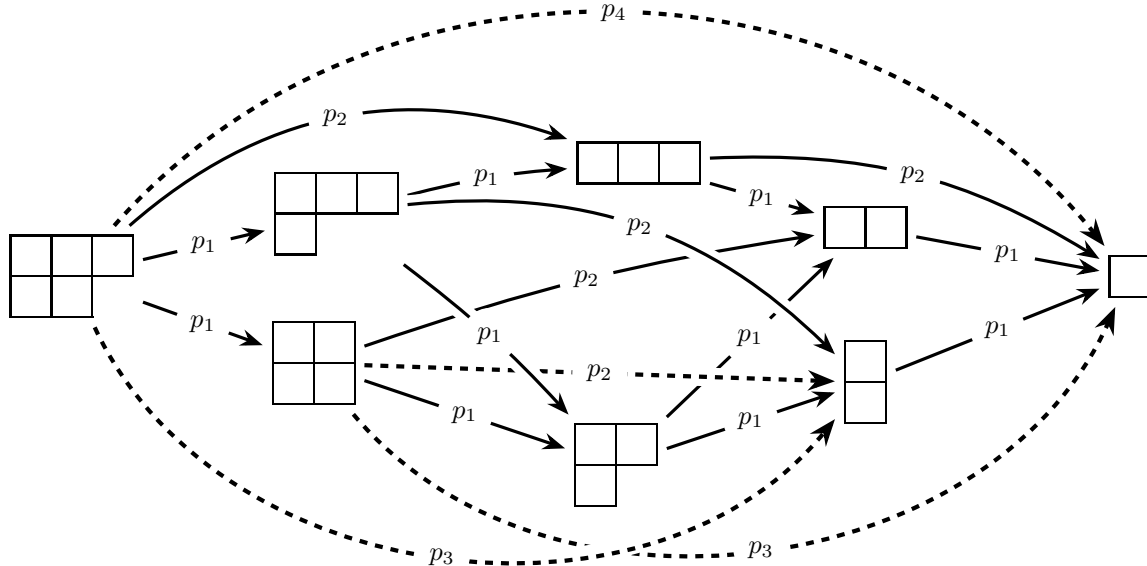


Figure 1: The diagrams for $\lambda = (3, 2)$ and those obtained by removal of border strips of size j , which is indicated by p_j . The solid and dashed lines again indicate the removal of border strips of even and odd heights, respectively. This graph indicates all ways to remove border strips from $(3, 2)$ and the resulting diagrams, except for those cases where the removal of a border strip leads to the empty diagram.

keeping in mind the sign given by $(-1)^{\text{ht}(\eta_j)}$ with $|\eta_j| = \alpha_j$. This gives the following.

$$\begin{aligned}
\langle s_{(3,2)} s_{(3,2)} \rangle_c &= \binom{(1)}{s_{(2,2)} + s_{(3,1)}}^2 + \frac{\binom{(2)}{1}{s_{(3)}}^2}{2} + \frac{\binom{(1^2)}{2s_{(2,1)} + s_{(3)}}^2}{2} + \frac{\binom{(3)}{1}{s_{(1^2)}}^2}{3} + \frac{\binom{(2,1)}{1}{s_{(2)}}^2}{2} \\
&+ \frac{\binom{(1^3)}{3s_{(2)} + 2s_{(1^2)}}^2}{3!} + \left(\frac{1}{3} + \frac{1}{8} + \frac{1}{4} + \frac{1}{4} + \frac{5^2}{4!} \right) s_{(1)} + 1. \tag{59}
\end{aligned}$$

The last two terms on the bottom line of the expression above arise from $|\alpha| = 4, 5$. In the latter case, following arrows indicated by p_{α_j} leads to \emptyset . One can see that there is only a single way to start at $\begin{smallmatrix} \square & \square & \square \\ \square & \square & \end{smallmatrix}$ and arrive at \emptyset for $\alpha = (4, 1), (3, 2), (3, 1^2), (2^2, 1), (2, 1^3)$ by following the corresponding arrows in the graph above. However, we already noted that there are 5 distinct ways $\begin{smallmatrix} \square & \square & \square \\ \square & \square & \end{smallmatrix}$ and arrive at \square following arrows with p_1 . This implies there are also 5 ways to arrive at \emptyset by removing single elements, simply by taking the additional step $\square \xrightarrow{p_1} \emptyset$. This gives

$$\frac{1}{z_{(4,1)}} + \frac{1}{z_{(3,2)}} + \frac{1}{z_{(3,1^2)}} + \frac{1}{z_{(2,1^3)}} + \frac{1}{z_{(2^2,1)}} + \frac{5^2}{z_{(1^5)}} = \frac{1}{4} + \frac{1}{6} + \frac{1}{6} + \frac{1}{12} + \frac{1}{8} + \frac{5^2}{5!} = 1, \tag{60}$$

leading to the unit contribution in equation (59). Via this reasoning, one may check that expression (59) and (58) are identical. The above example may not appear to give a very convincing argument in favor

of equation (52) over (257), as the application of (52) appears to be more complicated than (257) for the case of $\lambda = (3, 2)$. Indeed, for partitions containing few cells, such as $\lambda = (3, 2)$, it is convenient to use (257), as the skew partitions λ/ν can easily be related to non-skew partitions, as in (58). However, for larger partitions, this is no longer the case, as (188), (189), and (197) can no longer be applied. When considering larger partitions, then, equation (52) can still be used to express general objects $\langle s_\lambda s_\nu \rangle_c$ in terms of non-skew Schur polynomials. This will allow us to express complicated correlation functions in terms of simpler ones in section 3.2.3, but can be used more generally in situations where an expression for $\langle s_\lambda s_\nu \rangle$ in terms of non-skew Schur polynomials is desirable.

2.3.2 Expansion in power sum symmetric polynomials

For certain applications, such as the LRRW models we will be considering in the next section, expanding $\langle s_\lambda(U) s_\nu(U^{-1}) \rangle$ in terms of power sums $p_k(x)$ and $p_k(y)$ may be particularly useful. One way to do so is to use the expansion in (201), calculate all $\chi_\alpha^\lambda, \chi_\alpha^\nu$, and contract power sums using (7). However, this is rather inconvenient as the computation of all the symmetric group characters is rapidly becomes more complicated for larger λ, ν . Instead, it would be more effective to once more use equation (208) to find a recursive expansion in terms of power sum polynomials. We will do so here, ultimately leading to equation (68). For comparison, we will also consider the more complicated method that involves the calculation of all $\chi_\alpha^\lambda, \chi_\alpha^\nu$ at the end of this subsection to demonstrate its inconvenience compared to equation (68).

The expression that we will be deriving provides an iterative method for expanding in $p_\gamma(x)$ and $p_\omega(y)$ that does not require us to find χ_α^λ and χ_α^ν for all α and then contract over all combinations of power sum polynomials. Essentially, we apply equations (36) and (201) to $\langle s_\lambda(U) s_\nu(U^{-1}) \rangle$ and make use of the orthogonality properties of the symmetric group characters. In particular, we will revert the order of expansion in section 2.3.1 and start from the term with all p_μ contracted, see equation (54), then consider the term where a single p_j is not contracted, then two uncontracted power sums, and so on. For simplicity, we start by considering autocorrelation function up to the subleading term, which gives

$$\langle s_\lambda(U) s_\lambda(U^{-1}) \rangle = \sum_{\mu, \rho} \frac{\chi_\mu^\lambda \chi_\rho^\lambda}{z_\mu z_\rho} \langle p_\mu(U) p_\rho(U^{-1}) \rangle = 1 + \sum_{j \geq 1} \sum_{\mu} \frac{(\chi_\mu^\lambda)^2 m_j(\mu)}{z_\mu j} p_j(x) p_j(y) + \dots \quad (61)$$

where sum is over all μ containing a row of size j . We have $\mu = \rho$ since this is the only way to contract all of p_μ with p_ρ except for two copies of p_j (one from p_μ and the other from p_ρ). Using the recursive formula for χ_μ^λ in (208) and the orthogonality of symmetric group characters in (54), the rightmost term in equation (61) then gives

$$\sum_j \frac{1}{j^2} \sum_{\mu} \frac{\left(\sum_{\eta} (-1)^{\text{ht}(\eta)} \chi_{\mu-(j)}^{\lambda \setminus \eta} \right) \left(\sum_{\zeta} (-1)^{\text{ht}(\zeta)} \chi_{\mu-(j)}^{\lambda \setminus \zeta} \right)}{z_{\mu-(j)}} p_j(x) p_j(y) = \sum_{j \geq 1} \frac{p_j(x) p_j(y)}{j^2} \sum_{\eta} 1, \quad (62)$$

where η and ζ are border strips of size j . Equation (62) then tells us that the coefficient $p_j(x) p_j(y)$ in the power sum expansion of $\langle s_\lambda(U) s_\lambda(U^{-1}) \rangle$ is given by $\frac{1}{j^2}$ times the number of ways to remove a border strip of size j from λ . Consider another term in this expansion, where $\mu = (j, \alpha)$, $\rho = (k^2, \alpha)$ with $j = 2k$,

and contract over p_α leading to the term proportional to $p_j(x)p_k(y)^2$. Via the same reasoning as above, this is given by

$$\frac{p_j(x)p_k(y)^2}{2jk^2} \sum_{\eta,\zeta,\xi} (-1)^{\text{ht}(\eta)+\text{ht}(\zeta)+\text{ht}(\xi)} \delta_{\lambda \setminus \{\eta, (\lambda \setminus \zeta) \setminus \xi\}} , \quad (63)$$

where the sums are over all η , border strips of size j , and ζ and ξ , border strips of size k . We see that the terms appearing in the power sum expansion of $\langle s_\lambda(U)s_\lambda(U^{-1}) \rangle$ are found by removing border strips $\{\eta\}$ and $\{\zeta\}$ from λ such that $\lambda \setminus \{\eta\} = \lambda \setminus \{\zeta\}$. Continuing this procedure gives the following. Consider not contracting $p_\omega(U)$ and $p_\gamma(U^{-1})$ for some ω and γ , leading to the term proportional to $p_\omega(y)p_\gamma(x)$. In general this leads to a sum over μ and ρ (in the middle expression in (62)) of the form

$$\mu = (\omega, \alpha) \quad , \quad \rho = (\gamma, \alpha) \quad , \quad (64)$$

so that $m_j(\mu) - m_j(\omega) = m_j(\alpha) = m_j(\rho) - m_j(\gamma)$ for all j , and $|\omega| = |\eta|$. Since we sum over μ and ρ for a fixed choice of ω and γ , this effectively leads to a sum over α . Since there are $\frac{1}{m_j(\alpha)!} \frac{m_j(\mu)!}{m_j(\omega)!} \frac{m_j(\rho)!}{m_j(\gamma)!}$ ways to perform $m_j(\alpha)$ contractions of p_j appearing in p_μ and p_ρ , we have

$$\langle p_\mu p_\rho \rangle = \dots + p_\omega(y)p_\gamma(x) \prod_{j \geq 1} \frac{1}{m_j(\alpha)!} \frac{m_j(\mu)!}{(m_j(\mu) - m_j(\alpha))!} \frac{m_j(\rho)!}{(m_j(\rho) - m_j(\alpha))!} j^{m_j(\alpha)} + \dots \quad (65)$$

where we show only the term proportional to $p_\omega(y)p_\gamma(x)$. Using the fact that,

$$z_\mu = z_\alpha \prod_{j \geq 1} j^{m_j(\mu) - m_j(\alpha)} \frac{m_j(\mu)!}{m_j(\alpha)!} , \quad (66)$$

and again applying the orthogonality of symmetric group characters, we find that the term proportional to $p_\omega(y)p_\gamma(x)$ in the expansion of $\langle s_\lambda(U)s_\lambda(U^{-1}) \rangle$ is given by

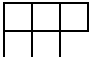
$$\frac{p_\omega(y)p_\gamma(x)}{z_\omega z_\gamma} \sum_{\{\eta\}, \{\xi\}} (-1)^{\text{ht}(T_\eta) + \text{ht}(T_\xi)} \delta_{\lambda \setminus \{\eta\}, \lambda \setminus \{\xi\}} , \quad (67)$$

where the sum is over border strips η_1, η_2, \dots satisfying $|\eta_j| = \omega_j$, as well as border strips ξ_j satisfying $|\xi_j| = \gamma_j$. Further, T_η and T_ξ are the (generally disconnected) skew diagrams consisting of the unions of the border strips in η and ξ , respectively, and $\text{ht}(T)$ is defined in (204). It is clear that the examples in (62) and (63) arise as special cases of (67). The autocorrelation function can then be expanded as a sum ω and γ , each contributing a term of the form appearing in (67). The same reasoning can evidently be applied to more general correlation functions, which are then given by

$$\boxed{\langle s_\lambda(U)s_\nu(U^{-1}) \rangle = \sum_{\omega, \gamma} \frac{p_\omega(y)p_\gamma(x)}{z_\omega z_\gamma} \sum_{\{\eta\}, \{\xi\}} (-1)^{\text{ht}(T_\eta) + \text{ht}(T_\xi)} \delta_{\lambda \setminus \{\eta\}, \nu \setminus \{\xi\}} .} \quad (68)$$

The above expression can be straightforwardly applied by considering the different ways to remove bor-

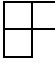
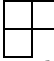
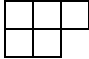
der strips from λ and ν such that the resulting diagrams are identical, as expressed by the presence of $\delta_{\lambda \setminus \{\eta\}, \nu \setminus \{\xi\}}$. This provides a recursive expression which significantly simplifies various computations, especially when λ, ν are large diagrams for which the computation of the symmetric group characters rapidly grows more difficult. Equation (68) is particularly useful for applications where one has access to $p_k(x)$ and $p_k(y)$. This includes LRRW models, where $p_k(x)$ and $p_k(y)$ are proportional to the time parameter and the hopping parameters, as we will see in the next section.

We now apply (68) to $\langle s_\lambda(U) s_\lambda(U^{-1}) \rangle$ for $\lambda = (3, 2)$. Consider all distinct ways to remove a border strip of size one, i.e. a single cell, from . As can be seen in figure 1, this results in the following diagrams.

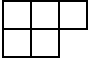
$$\begin{array}{cc}
 \begin{array}{|c|c|c|} \hline \square & \square & \blacksquare \\ \hline \square & \square & \\ \hline \end{array} &
 \begin{array}{|c|c|c|} \hline \square & \square & \square \\ \hline \square & \blacksquare & \\ \hline \end{array} \\
 \end{array} \tag{69}$$

Removing a single cell twice results in the following diagrams.

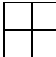
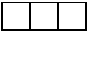
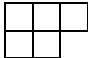
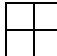
$$\begin{array}{cc}
 \begin{array}{|c|c|c|} \hline \square & \square & \square \\ \hline \blacksquare & \blacksquare & \\ \hline \end{array} & 2 \begin{array}{|c|c|c|} \hline \square & \square & \blacksquare \\ \hline \square & \blacksquare & \\ \hline \end{array} \\
 \end{array} \tag{70}$$

We get multiplicity two for  on the right as one can remove the single cells indicated in black in either order, corresponding to the fact that there are two distinct ways to arrive at  from  by following p_1 in figure 1. Removing border strips of sizes 2, 3, 4 results in the diagrams below.

$$\begin{array}{ccc}
 \begin{array}{|c|c|c|} \hline \square & \square & \square \\ \hline \blacksquare & \blacksquare & \\ \hline \end{array} &
 \begin{array}{|c|c|c|} \hline \square & \blacksquare & \blacksquare \\ \hline \square & \blacksquare & \\ \hline \end{array} &
 \begin{array}{|c|c|c|} \hline \square & \blacksquare & \blacksquare \\ \hline \blacksquare & \blacksquare & \\ \hline \end{array} \\
 \end{array} \tag{71}$$

Note that the height ht of the border strips of sizes 3 and 4 is given by 1, so that $(-1)^{ht} = -1$. It is easy to see that no border strips of size ≥ 5 can be removed from , since it is a partition of 5 that is not itself a border strip. From the fact that there are two distinct ways to remove a single cell from λ , and only a single way to remove border strips of sizes 2, 3, 4, we see that the corresponding contributions are given by

$$2p_1(x)p_1(y) + \frac{p_2(x)p_2(y)}{4} + \frac{p_3(x)p_3(y)}{9} + \frac{p_4(x)p_4(y)}{16} . \tag{72}$$

Consider now the term proportional to $p_1(x)^2 p_1(y)^2$. The two diagrams which arise from consecutively removing two single cells are  and , where the former appears with multiplicity two, as demonstrated above. We thus see that there are four ways to take two copies of , consecutively remove two single cells, and end up with . Conversely, there is only a single way to end up with

$\square\square\square$ via this procedure. Combined with $(z_{(1^2)})^2 = 4$, this demonstrates that we have

$$\frac{5p_1(x)^2p_1(y)^2}{4} \quad (73)$$

appearing in the expansion of $\langle s_{(3,2)}s_{(3,2)} \rangle$. Lastly, we consider $p_2(x)p_1(y)^2 + p_1(x)^2p_2(y)$. One may remove either a border strip of size two or two single cells and end up in $\square\square\square$, see the leftmost diagrams in (70) and (71). Combined with $z_{(1^2)} = 2 = z_{(2)}$, this results in

$$\frac{p_2(x)p_1(y)^2 + p_1(x)^2p_2(y)}{4}. \quad (74)$$

Although the effectiveness of (68) is already clear for $\begin{array}{|c|c|c|} \hline \square & \square & \square \\ \hline \square & & \\ \hline \end{array}$, this is still a rather

small partition. For larger λ , it becomes progressively harder to compute χ^λ_α , increasing the advantage of (68). We will work out more complicated examples in section 3.2.4, where we apply the above results to correlation functions of LRRW models.

We now proceed to compute $\langle s_{(3,2)}(U)s_{(3,2)}(U^{-1}) \rangle$ via the more laborious method briefly outlined at the start of this subsection, where we compute $\chi^\lambda_\alpha^{(3,2)}$ for all α , apply (201), and perform all possible contractions between the power sum polynomials appearing in (201). We will see in the following section, below equation (134), that one may calculate χ^λ_α by using a relation with fermionic particles hopping on a one-dimensional lattice. One may then apply Wick's theorem to the resulting expression to find an expansion of LRRW correlation functions in terms of power sums. Although this may provide a convenient method for calculating χ^λ_α , we will see here that its application to the computation of $\langle s_\lambda(U)s_\nu(U^{-1}) \rangle$ is much less convenient than simply applying equation (68). Using (208) and looking at figure 1, we see that the non-zero characters χ^λ_α are given by

$$\begin{aligned} \chi_{(1^5)}^{(3,2)} &= 5, & \chi_{(2,1^3)}^{(3,2)} &= 1, & \chi_{(2^2,1)}^{(3,2)} &= 1, \\ \chi_{(3,1^2)}^{(3,2)} &= 1, & \chi_{(3,2)}^{(3,2)} &= -1, & \chi_{(4,1)}^{(3,2)} &= 1. \end{aligned} \quad (75)$$

Applying (201) gives

$$\begin{aligned} s_{(3,2)} &= \frac{p_1^5}{24} + \frac{p_1^3p_2}{12} + \frac{p_1^2p_3}{6} + \frac{p_2^2p_1}{8} - \frac{p_2p_3}{6} + \frac{p_1p_4}{4} \\ &= \frac{P(1^5)}{24} + \frac{P(2,1^3)}{12} + \frac{P(3,1^2)}{6} + \frac{P(2^2,1)}{8} - \frac{P(3,2)}{6} + \frac{P(4,1)}{4}. \end{aligned} \quad (76)$$

We then apply Wick's theorem to $\langle s_{(3,2)}(U)s_{(3,2)}(U^{-1}) \rangle_c$. We give three examples below, again indicating the compositions α corresponding to the p_α which are contracted.

$$\begin{aligned} \frac{1}{4}p_1^{(4)}(x)p_1(y) + \frac{1}{8}p_1^{(2^2)}(x)p_1(y) + \frac{3}{6^2}(p_2^{(3)}(x)p_2(y) - p_2(y)p_1(x)^2) + \\ + \frac{3}{6^2}(p_1(x)^2p_1(y)^2 - p_2(x)p_1(y)^2) + \dots \end{aligned} \quad (77)$$

We will use the above method to find the prefactors of $p_\omega(y)p_\gamma(x)$ for some examples of ω, γ . Consider first $\gamma = \omega = (4)$, leading to a term proportional to $p_4(x)p_4(y)$. This term is rather simple to find as we only get a contribution from the rightmost term in (76). In particular, we have

$$\frac{1}{4^2} \langle p_{(4,1)}(U)p_{(4,1)}(U^{-1}) \rangle_c = \frac{p_4(x)p_4(y)}{4^2} + \frac{p_1(x)p_1(y)}{4} + \frac{1}{4}, \quad (78)$$

so that $p_4(x)p_4(y)$ appears with a prefactor $\frac{1}{4^2}$ in the expansion of $\langle s_{(3,2)}(U)s_{(3,2)}(U^{-1}) \rangle$. We consider now those terms proportional to $p_3(x)p_3(y)$ arising from (76), where the dots below refer to terms not proportional to $p_3(x)p_3(y)$ and where we omit writing $(U^{\pm 1})$ explicitly henceforth.

$$\begin{aligned} \frac{1}{6^2} \langle p_{(3,1^2)}p_{(3,1^2)} \rangle + \frac{1}{6^2} \langle p_{(3,2)}p_{(3,2)} \rangle &= \frac{p_3(x)p_3(y)}{36}(2+2) + \dots \\ &= \frac{p_3(x)p_3(y)}{9} + \dots \end{aligned} \quad (79)$$

For $p_2(x)p_2(y)$, we find

$$\begin{aligned} \frac{\langle p_{(2,1^3)}p_{(2,1^3)} \rangle}{(12)^2} + \frac{\langle p_{(2^2,1)}p_{(2^2,1)} \rangle}{8^2} + \frac{\langle p_{(3,2)}p_{(3,2)} \rangle}{6^2} &= p_2(x)p_2(y) \left(\frac{3!}{12} + \frac{8}{8^2} + \frac{3}{6^2} + \dots \right) \\ &= \frac{p_2(x)p_2(y)}{4} + \dots \end{aligned} \quad (80)$$

We see a pattern emerge as we get $\frac{p_i(x)p_i(y)}{j^2}$ for all j considered thus far. However, this pattern does not continue down to $j = 1$. In particular, the following expression

$$\frac{\langle p_{(1^5)}p_{(1^5)} \rangle}{(24)^2} + \frac{\langle p_{(2,1^3)}p_{(2,1^3)} \rangle}{(12)^2} + \frac{\langle p_{(3,1^2)}p_{(3,1^2)} \rangle}{6^2} + \frac{\langle p_{(2^2,1)}p_{(2^2,1)} \rangle}{8^2} + \frac{\langle p_{(4,1)}p_{(4,1)} \rangle}{4^2}, \quad (81)$$

is given by

$$p_1(x)p_1(y) \left(\frac{(5!)^2}{(4!)^3} + \frac{6^2}{(12)^2} + \frac{12}{6^2} + \frac{8}{8^2} + \frac{4}{4^2} \right) + \dots = 2p_1(x)p_1(y) + \dots \quad (82)$$

Combining equations (78), (79), (80), and (82) then leads to equation (72), albeit via a much less convenient method.

Consider now the term proportional to $p_1(x)^2p_1(y)^2$, which receives contributions from

$$\frac{\langle p_{(1^5)}p_{(1^5)} \rangle}{(24)^2} + \frac{\langle p_{(2,1^3)}p_{(2,1^3)} \rangle}{(12)^2} + \frac{\langle p_{(3,1^2)}p_{(3,1^2)} \rangle}{6^2}. \quad (83)$$

In particular, this contributes

$$p_1(x)^2p_1(y)^2 \left(\frac{(5!)^2}{(4!)^2(2!)^23!} + \frac{(12)^2}{12} + \frac{3}{6^2} \right) = \frac{5p_1(x)^2p_1(y)^2}{4}, \quad (84)$$

thus confirming equation (73). Lastly, we consider a mixed term, namely, the term proportional to

$p_2(x)p_1(y)^2 + p_1(x)^2p_2(y)$. This is given by

$$\begin{aligned} \frac{\langle p_{(1^5)}p_{(2,1^3)} \rangle}{12 \cdot 24} - \frac{\langle p_{(3,1^2)}p_{(3,2)} \rangle}{6^2} + \frac{\langle p_{(2,1^3)}p_{(2^2,1)} \rangle}{12 \cdot 8} &= p_2(x)p_1(y)^2 \left(\frac{5}{24} - \frac{1}{12} + \frac{1}{8} \right) + \dots \\ &= \frac{p_2(x)p_1(y)^2}{4} + \dots \end{aligned} \quad (85)$$

Of course, inverting the order of $p_\mu(U)$ and $p_\rho(U^{-1})$ in $\langle p_\mu(U)p_\rho(U^{-1}) \rangle$ above gives the same contribution with $x \leftrightarrow y$. The end result is therefore $\frac{p_2(x)p_1(y)^2 + p_1(x)^2p_2(y)}{4}$, thereby confirming (74). It is clear from this simple example that the method applied in the second part of this subsection is much less powerful than equation (68), and this becomes more acute when we consider larger partitions than $\lambda = (3, 2)$ as the χ_α^λ are then a lot harder to compute.

3 Applying symmetric polynomial theory to long-range random walks

We will now apply some of the results above to LRRW correlation functions by using their relation to weighted $U(N)$ integrals over Schur polynomials in equation (237) and identities from symmetric polynomial theory, as well as results we derived in section 2. We first consider identities relating to elementary and complete homogeneous symmetric polynomials, before moving on to power sum polynomials and border strips. We will generally take $N \rightarrow \infty$ here, although the presentation in sections 3.1.1, 3.2.1, and 3.2.2 is valid for finite N as well.

3.1 Elementary and complete homogeneous symmetric polynomials

We repeat here the expression for the weight function in (228),

$$f(e^{i\theta}; \tau) = \exp \left(\tau \sum_{k \in \mathbb{Z}} a_k e^{i\theta} \right), \quad (86)$$

where a_k are the hopping parameters of the hamiltonian in (225). As noted before, the hamiltonian is a Toeplitz matrix, and a_k is the number on its k^{th} diagonal. By comparing with (161), we see that we can write the weight function as

$$f(z) = H(x; z)H(y; z^{-1}), \quad (87)$$

with the following identification, for $k \geq 1$,

$$\begin{aligned} \tau a_k &= \frac{p_k(x)}{k}, \\ \tau a_{-k} &= \frac{p_k(y)}{k}. \end{aligned} \quad (88)$$

Alternatively, we can write

$$f(z) = E(x; z)E(y; z^{-1}) , \quad (89)$$

by identifying, for $k \geq 1$,

$$\begin{aligned} \tau a_k &= \frac{(-1)^{k+1} p_k(x)}{k} , \\ \tau a_{-k} &= \frac{(-1)^{k+1} p_k(y)}{k} , \end{aligned} \quad (90)$$

and by transposing the diagrams as in (258). When $\tau \rightarrow 0$, i.e. the CUE limit, we have

$$F_{\lambda; \mu}(0) = \langle s_\lambda(U) s_\mu(U^{-1}) \rangle_{\text{CUE}} = \delta_{\lambda, \mu} , \quad (91)$$

which is again simply the orthonormality of Schur polynomials as the irreducible characters of $U(N)$. By using the strong Szegő limit theorem, we can compute $F_{\emptyset; \emptyset}$ ¹. Assuming $a_0 = 0$, i.e. zero on-site energy, we have

$$F_{\emptyset; \emptyset}(\tau) = \exp \left(\tau^2 \sum_{k=1}^{\infty} k a_k^2 \right) . \quad (92)$$

If we have $a_0 \neq 0$, we get an additional multiplicative term $e^{-N\tau a_0}$ on the right, where one should remember that we take $N \rightarrow \infty$. Considering $a_1 = -1 = a_1$ and $a_k = 0$ otherwise, i.e. the XX0-model, and choosing $\tau = it$, we recover the result of [46] and [45], see also [47],

$$F_{\emptyset; \emptyset}(it) = e^{-t^2} . \quad (93)$$

Remember that equations (256) and (257) state that

$$F_{\lambda; \mu}(\tau) = F_{\emptyset; \emptyset}(\tau) \langle s_\lambda(U) s_\mu(U^{-1}) \rangle_\tau , \quad (94)$$

where $\langle \dots \rangle_\tau$ is given in equation (249) with weight function given by $f(z; \tau)$ in (228). We therefore define

$$G_{\lambda; \mu}(\tau) := \frac{F_{\lambda; \mu}(\tau)}{F_{\emptyset; \emptyset}(\tau)} = \langle s_\lambda(U) s_\mu(U^{-1}) \rangle_\tau , \quad (95)$$

i.e. we express correlations in terms of their proportionality to $F_{\emptyset; \emptyset}(\tau)$. We will also write this as

$$G_{\lambda; \mu}(\tau) =: \langle \lambda | \mu \rangle_\tau . \quad (96)$$

If $\mu = \emptyset$ (or $\lambda = \emptyset$), we will simply write

$$G_{\lambda; \emptyset}(\tau) = \langle \lambda | \emptyset \rangle_\tau =: \langle \lambda \rangle_\tau . \quad (97)$$

¹This has been noted before, see e.g [45].

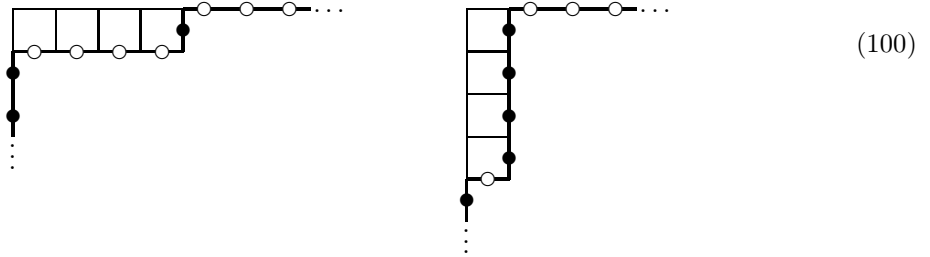
We also define the following - connected - correlation function,

$$G_{\lambda;\mu}^c(\tau) =: \langle \lambda | \mu \rangle_\tau - \langle \lambda \rangle_\tau \langle \mu \rangle_\tau^* . \quad (98)$$

We consider now some explicit examples. Using (167), we can express

$$\langle e_n \rangle_\tau = e_n(y) = G_{(1^n);\emptyset} , \quad \langle h_n \rangle_\tau = h_n(y) = G_{(k);\emptyset} , \quad (99)$$

and their complex conjugates $G_{\emptyset;(1^n)}$ and $G_{\emptyset;(n)}$, in terms of $p_k(y)$ with $k \leq n$. For h_n and e_n with $n = 4$, the diagrams and corresponding configurations are given below on the left and right, respectively.



That is, h_n correspond to taking only the single rightmost particle and moving it n sites to the right, whereas e_n corresponds to taking the n rightmost particles and moving them all a single site to the right. Note that with $x = (x_1, \dots, x_K)$, we have $e_j(x) = 0$ for $j > K$ (and likewise for y). This means that, for any $n, m > K$,

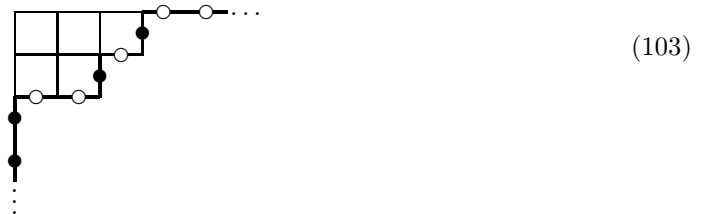
$$F_{(1^m);(1^n)} = \sum_{j=0}^K e_j e_j \quad (101)$$

That is, when we move $n > K$ adjacent particles by a single site, the effect is the same as to move K adjacent particles a single site.

Not only can we read off $G_{(n);\emptyset}$ and $G_{(1^n);\emptyset}$ (and their complex conjugates). From the corollary of the Pieri formula in (188), we have that, for any λ ,

$$G_{\lambda;(n)}^c = \langle s_\lambda(U) h_n(U^{-1}) \rangle_c = \sum_{j=1}^n h_{n-j} s_{\lambda/(j)} = \sum_{j=1}^n h_{n-j} \sum_{\nu^j} s_{\nu^j} , \quad (102)$$

where the rightmost sum is over all ν^j such that λ/ν^j is a horizontal strip of length j . Take, for example, $\lambda = (3, 2)$,



which corresponds to

$$|(3, 2)\rangle = \cdots \bullet \bullet \circ \circ \bullet \circ \bullet \circ \bullet \circ \cdots \quad (104)$$

We remind the reader that the dots on the left (right) refer to an infinite string of particles (holes). We take $\lambda = (3, 2)$ and $n = 2$. For this choice of λ , the diagrams contributing to the sum over ν^1 and ν^2 in (102) are given in equation (69).

We assign particles and holes to these diagrams and remind ourselves that

$$G_{(1);\emptyset}(\tau) = \langle \cdots \bullet \circ \bullet \circ \cdots \rangle_{\tau} \quad (105)$$

We then see that equation (102) is given by the following expression. For each configuration, the dots on the left and right again indicate an infinite sequence of particles and holes, of which we show only the left- and rightmost, respectively.

$$\begin{aligned} G_{(3,2);(2)}(\tau) &= \langle \cdots \bullet \circ \circ \bullet \circ \bullet \circ \cdots \mid \cdots \bullet \circ \circ \bullet \circ \cdots \rangle_{\tau} \\ &= \left(\langle \cdots \bullet \circ \circ \bullet \bullet \circ \cdots \rangle_{\tau} + \langle \cdots \bullet \circ \bullet \circ \circ \bullet \circ \cdots \rangle_{\tau} \right) \times G_{(1);\emptyset}(\tau) \\ &\quad + \langle \cdots \bullet \circ \bullet \circ \bullet \circ \cdots \rangle_{\tau} + \langle \cdots \bullet \circ \circ \circ \bullet \circ \cdots \rangle_{\tau} \end{aligned} \quad (106)$$

The second line above corresponds to ν^1 in (102), whereas the third line corresponds to ν^2 . By comparing with equation (103), we see that the sum over ν^1 contains all diagrams related to $\begin{array}{|c|c|c|} \hline \square & \square & \square \\ \hline \square & & \\ \hline \end{array}$ by moving a single particle a single site to the left. The sum over ν^2 consists of all ways to move one or two particles by a total of two sites, with the restriction that we cannot move two adjacent particles. This is the interpretation of the corollary of the Pieri formula in (188), and it generalizes to h_n for any $n \in \mathbb{Z}^+$. In particular, we can assign a particle-hole interpretation to $s_{\lambda/(1^n)}$ by noting that it is given by summing over all distinct ways to move $\leq n$ particles a total of n sites to the left without moving any two adjacent particles. We can apply the same reasoning to $\langle s_{\lambda}(U)e_n(U^{-1}) \rangle$ by using (189). Similar to (102), we have

$$G_{\lambda;(1^n)} = \sum_{j=1}^n e_{n-j} s_{\lambda/(1^j)} = \sum_{j=1}^n e_{n-j} \sum_{\nu^j} s_{\nu} , \quad (107)$$

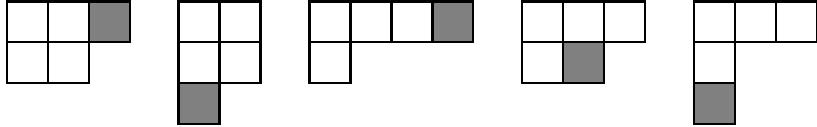
where \sum_{ν^j} is now a sum over all ν such that λ/ν is a vertical strip of length j . The skew Schur polynomial $s_{\lambda/(1^n)}$ can be interpreted as taking the configuration corresponding to λ and summing over all distinct ways to move n particles a single site to the left.

Consider the case where $x = y$ (e.g. $\tau = \beta \in \mathbb{R}$ and $a_k = a_{-k}$). We can then apply the Pieri formula once

again, in this case to the products $h_{n-j}s_{\lambda/(j)}$ in (102), as

$$h_{n-j}s_{\lambda/(j)} = \sum_{\nu} s_{\nu} , \quad (108)$$

where the sum is over all ν obtained from λ by removing a horizontal strip of size j and then adding to the resulting diagram a horizontal strip of size $n - j$. We consider again $G_{(3,2);(2)} = s_{(3,2)/(1)}h_1 + s_{(3,2)/(2)}$, where $(3,2)/(2) = (2,1) + (3)$. Applying the Pieri formula to $s_{(3,2)/(1)}h_1 = s_{(3,2)/(1)}s_{(1)}$ gives the following diagrams, where the cell that is added again indicated in gray. It is clear that $\lambda = (3,2)$ appears twice, as there are two ways to remove (and then add again) a single cell from λ .


(109)

We now briefly consider the single particle correlation functions $F_{j;l}$. The generating function $f(z) = \sum_j F_{j;l}z^{j-l}$ for one-particle correlations is written in (228). Writing again $f(z) = H(x;z)H(x;z^{-1})$ for some x , we have

$$f(z) = \prod_j (1 - x_j z)^{-1} (1 - y_j z^{-1})^{-1} = \sum_{j,k=0}^{\infty} h_j(x) h_k(y) z^{j-k} =: \sum_{m=0}^{\infty} d_m (z^m + z^{-m}) , \quad (110)$$

where h_j are complete homogeneous symmetric polynomials. Then,

$$d_m = \sum_{j=m}^{\infty} h_j(y) h_{j-m}(x) = \langle h_M(U) h_{M-m}(U^{-1}) \rangle = G_{j;l}(\tau) , \quad j - l = m . \quad (111)$$

where M is the largest number k such that $h_k \neq 0$, which is typically infinite. Remember that the $G_{j;l}(\tau)$ are the single-particle wavefunctions at site j and time τ for a particle released from site l . The last two equalities in (111) relate $F_{j;l}(\tau)$ to single-particle wavefunctions at site M and time τ for a particle released from site $M - m$. Since M is infinite for most choices of hopping parameters $a_k \sim p_k$, this correspond to releasing a particle at infinity and finding its wavefunction m lattice sites away from where it was released at some Euclidean time τ . The fact that $h_{M-m}(U^{-1}) = G_{j;l}(\tau)$ for $M \rightarrow \infty$ agrees with the intuition that a single particle at infinity does not feel the presence of the other remaining particles, which are infinitely far away from it.

Lastly, we note that one can apply the Jacobi-Trudi identity (200) to h_n and e_n to find any skew Schur polynomials on the right hand side of (257). This, in effect, provides a way to compute any correlation function. Although the resulting expressions generally grow quickly as one considers large partitions, the application of this method itself is rather simple as it only requires the computation of a determinant. In 3.2, we will outline various other, closely interrelated, methods to calculate any $\langle s_{\lambda} s_{\mu} \rangle$, based on power sum polynomials rather than elementary and complete homogeneous symmetric polynomials.

3.1.1 Quasi-local particle-hole duality

Remember that one can replace the generating function $f_1(z) = H(x; z)H(y; z^{-1})$ by $f_2(z) = E(x; z)E(y; z^{-1})$ at the cost of transposing the partitions appearing in the correlation functions. This leads to a duality between models related by $a_n \rightarrow (-1)^{n+1}a_n$, as we demonstrate here. Though mathematically trivial, the physical interpretation of this duality is quite surprising. As mentioned at the start of this section, this duality holds for finite as well as infinite N . From (161), it follows that switching between $f_1(z)$ and $f_2(z)$ corresponds to taking

$$p_k(x) \rightarrow (-1)^{k+1}p_k(x) . \quad (112)$$

From equations (88) and (90), it is clear that replacing as $p_k(x) \rightarrow (-1)^{k+1}p_k(x)$ corresponds to $a_k \rightarrow (-1)^{k+1}a_k$. In particular, we consider two hamiltonians for the same a_n ,

$$\begin{aligned} \hat{H}_1 &= - \sum_{m=0}^{\infty} \sum_n a_n (\sigma_m^- \sigma_{m+n}^+ + \sigma_m^- \sigma_{m-n}^+) , \\ \hat{H}_2 &= - \sum_{m=0}^{\infty} \sum_n (-1)^{n+1} a_n (\sigma_m^- \sigma_{m+n}^+ + \sigma_m^- \sigma_{m-n}^+) . \end{aligned} \quad (113)$$

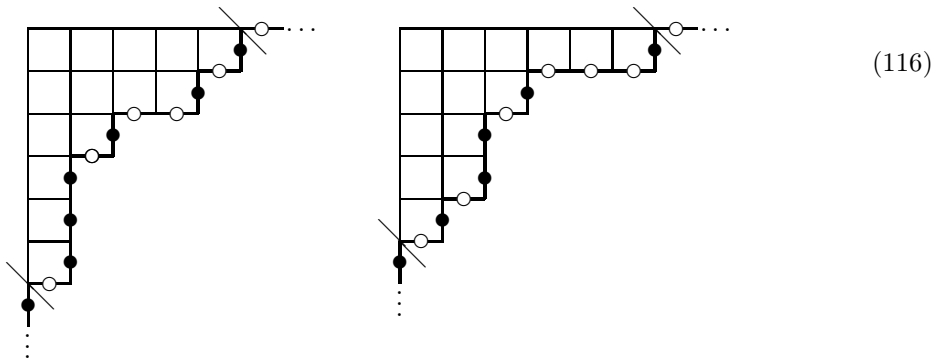
Correlation functions for \hat{H}_1 correspond to weight function $f_1(z)$, whereas those for \hat{H}_2 correspond to $f_2(z)$. Let us compare correlation functions for \hat{H}_1 and \hat{H}_2 , which we will write as $F_{\lambda; \mu}^{(1)}(\tau)$ and $F_{\lambda; \mu}^{(2)}(\tau)$, respectively. From Szegő's theorem, we know that $F_{\emptyset; \emptyset}$ only depends on $p_k(x)p_k(y)$, so taking $p_k \rightarrow (-1)^{k+1}p_k$, has no effect on $F_{\emptyset; \emptyset}$. Therefore,

$$F_{\emptyset; \emptyset}^{(1)}(\tau) = F_{\emptyset; \emptyset}^{(2)}(\tau) , \quad (114)$$

that is, the return probability for N adjacent particles for \hat{H}_1 is identical to that of \hat{H}_2 for any τ . Moreover, by comparing (257) and (258), we see that, for general λ and μ ,

$$\boxed{F_{\lambda; \mu}^{(1)}(\tau) = F_{\lambda^t; \mu^t}^{(2)}(\tau) .} \quad (115)$$

This establishes the following duality between correlations functions of \hat{H}_1 and \hat{H}_2 . It is well known that transposition of diagrams induces a particle-hole and parity transformation on the corresponding particle-hole configuration. This simply follows from the fact that transposition exchanges left and right, and that it maps vertical edges to horizontal ones (and vice versa). However, we are not implementing particle-hole symmetry in (115) but instead we establish an equality between different correlation functions corresponding to different models. Let us consider the configuration associated to $\lambda = (5, 4, 2, 1^3)$ and $\lambda^t = (6, 3, 2^2, 1)$, given on the left and right below, respectively.



These correspond to the following configurations,

$$\begin{aligned}
 |\lambda\rangle &= \dots \left| \bullet \circ \bullet \bullet \bullet \circ \circ \bullet \circ \bullet \right| \dots , \\
 |\lambda^t\rangle &= \dots \left| \bullet \circ \bullet \circ \bullet \bullet \circ \bullet \circ \circ \bullet \right| \dots .
 \end{aligned} \tag{117}$$

where the vertical lines on the left and right correspond to the diagonal lines at the lower left and upper right corners of λ and λ^t in (116), respectively. We see that the regions in between the vertical lines for $|\lambda\rangle$ and $|\lambda^t\rangle$ are related by performing a parity transformation and exchanging between particles and holes. Only a finite interval $\ell(\lambda) \leq r \leq \lambda_1$ is affected non-trivially by this combination of particle-hole and parity transformations. We thus establish a bijection between the correlation functions corresponding to \hat{H}_1 and \hat{H}_2 , given by the transposition of diagrams, which we refer to as *quasi-local particle-hole duality*. It follows trivially from the above treatment that if $a_{2k} = 0$, $\forall k \in \mathbb{Z}^+$, then $H(x; z) = E(x; z)$, as can be seen immediately from (161). It follows that when all even hopping parameters a_{2k} are zero, we have $F_{\lambda; \mu}^{(1)} = F_{\lambda; \mu}^{(2)}$, so we can suppress the superscript. In this case, it follows from (115) that

$$F_{\lambda; \mu}(\tau) = F_{\lambda^t; \mu^t}(\tau) . \tag{118}$$

That is, any system with $a_{2k} = 0$ satisfies quasi-local particle-hole duality with itself.

3.2 Power sum symmetric polynomials and border strips

We consider now the particle-hole configurations corresponding to power sum polynomials p_k , which are a very natural basis for the application to LRRW models due to their proportionality to τa_k . Consider specifically the case where $\tau = it$. Then, from (88), we have

$$p_k(y) = -itka_k^* = (-p_k(x))^* = e^{i\phi} p_k(x) , \quad \phi := \pi - 2 \arg(p_k(x)) . \tag{119}$$

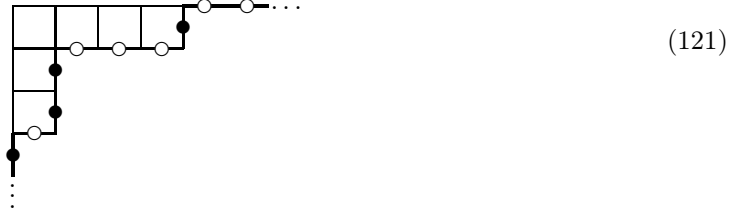
Since $p_k(x)$ only differs from $p_k(y)$ by a phase, we can apply the usual multiplication rules to objects of the form $p_\rho(x)p_\mu(y)$, which is an advantage over the usage of h_j, e_j .

Remember that power sum polynomials are expanded as an alternating sum over hook-shaped Schur

polynomials, see equation (175). Note that

$$\langle \text{tr} U^n \rangle_\tau = p_n = \sum_{r=0}^{n-1} (-1)^r G_{(n-r, 1^r); \emptyset}, \quad (120)$$

can be read off from the hamiltonian by the identification in either (88) or (90). As an example, the configuration corresponding to a hook shape $\lambda = (4, 1^2)$ is as follows.



That is, a hook-shaped diagram corresponds to taking the particle at site $-b$ and moving it $a + b$ sites to the right. More generally, consider

$$\langle p_n | s_\lambda \rangle = \sum_{r=0}^{n-1} (-1)^r G_{\lambda; (n-r, 1^r)}^c = \sum_{r=0}^{n-1} (-1)^r \langle (n-1, 1^r) | \lambda \rangle. \quad (122)$$

Using equation (197), this is given by

$$\sum_{r=0}^{n-1} (-1)^r s_{\lambda / (n-r, 1^r)} = \sum_{\eta} (-1)^{\text{ht}(\eta)} s_{\lambda \setminus \eta}, \quad (123)$$

where the sum is over all η which are border strips of size n , see e.g. the example in (18) for $n = 4$. Note that there is only a single Schur polynomial appearing on the right hand side, as opposed to (102) and (107), which contain factors of e_{n-j} and h_{n-j} , respectively. We consider a few specific examples of (123), already noted in [40], before treating it in generality. In particular, consider $\langle s_\lambda p_n \rangle_c$ with $(n-r, 1^r) \not\subseteq \lambda \forall r \in \{0, \dots, n-1\}$, such that $\lambda_1 + \lambda_1^t - 1 < n$. This gives

$$\langle \text{tr} U^{-n} \text{tr}_\lambda U \rangle_c = 0. \quad (124)$$

Writing λ in Frobenius notation as $\lambda = (a_1, \dots, a_k | b_1, \dots, b_k)$ with a_j satisfying $a_1 > \dots > a_k$ and similar for b_j . In this case, $a_1 + b_1 + 1$ equals the hook-length of the top left cell of λ . Equation (124) then states that $\langle \text{tr} U^{-n} \text{tr}_\lambda U \rangle_c = 0$ if $a_1 + b_1 + 1 < n$. In terms of particle-hole configurations, (124) states that $\sum_{r=0}^{n-1} (-1)^r G_{\lambda; (n-r, 1^r)}^c = 0$ if n is greater than the distance (in units of lattice spacing) between the leftmost hole and rightmost particle in the configuration corresponding to λ .

Further, write $m = a_1 + b_1 + 1 - n$ and consider $\lambda = (a|b) = (a_1, \dots, a_k | b_1, \dots, b_k)$ such that $m \leq a_1 - a_2 - 1$ and $m \leq b_1 - b_2 - 1$, respectively. Take $\mu = (a_2, \dots, a_k | b_2, \dots, b_k)$, obtained by removing the first row and

column from λ . Any $(n-r, 1^r) \subseteq \lambda$ then satisfies

$$\lambda/(n-r, 1^r) = (a_1 + 1, 1^{b_1})/(n-r, 1^r) \otimes \mu = (a_1 + 1 - n + r) \otimes (1^{b_1-r}) \otimes \mu. \quad (125)$$

Consider the example of $(6, 4, 3, 1^2)/(5, 1^3)$, which is given by the diagram below.



We then apply (162) to find

$$\langle s_\lambda(U) \text{tr} U^{-n} \rangle_c = \sum_{r=n-a_1-1}^{b_1} (-1)^r s_{\lambda/(n-r, 1^r)} = \pm s_\mu \sum_{k=0}^m (-1)^k h_{m-k} e_k = 0. \quad (127)$$

Assigning particle-hole configurations to the diagrams above, we see that the correlation function corresponding to $\langle s_\lambda(U) \text{tr} U^{-n} \rangle_c$ vanishes when the distance between the leftmost hole and rightmost particle, as well as the distance between the rightmost particle and the second-to-rightmost particle (and vice versa for holes), are sufficiently small compared to n .

We now consider (123) more generally. In this expression, ν is related to λ by the removal of a border strip, i.e. a connected skew diagram not containing a subdiagram that is a 2 by 2 block. In terms of particle-hole configurations, a 2 by 2 block corresponds to moving two adjacent particles by two sites to the right, see below.



In equation (123), the fact that a border strip has no 2 by 2 subdiagram therefore states that (the configuration corresponding to) ν is related to λ by moving (a) particle(s) left by n sites without moving two or more adjacent particles by two or more sites. The number of rows that λ/ν occupies (which is $\text{ht}(\lambda/\nu) + 1$) equals the number of particles that are involved in this process, which follows immediately from the fact that vertical edges on the boundary of a diagram correspond to particles. From the fact that the border strip is connected, it follows that it occupies only consecutive rows. For example, the skew diagram on the left is a border strip, whereas the one on the right clearly is not.

(129)

This means that only consecutive (but not necessarily adjacent) particles are affected. However, connect- edness is a stronger condition, and in the case of border strips this leads to the following observation. For a skew diagram λ/ν , we call the *outer rim* the (horizontal and vertical) edges on the bottom right of the diagram of λ/ν , as in e.g. [41]. Conversely, the *inner rim* consists of the edges on the top left of λ/ν . For a border strip containing n cells, we number the edges of the inner and outer rims by $j = \{1, \dots, n + 1\}$. We will refer to the j^{th} edge on the outer rim as the j^{th} outer edge, and likewise for the inner rim. We consider an explicit example, where $\lambda = (8, 6^2, 4, 1)$ and $\nu = (5^2, 3, 2, 1)$, leading to a border strip of size $n = 9$ below. On the right hand side, we number the vertical edges of the inner and outer rims of λ/ν .

(130)

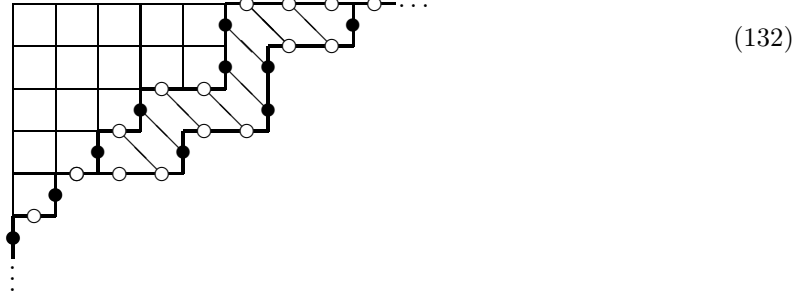
One can see in the above example that the first edge on the inner rim and the ledge edge on the outer rim are both vertical, which is clearly true for any (skew) diagram. Further, we see that all other vertical edges occupy the same positions on the inner and outer rims, namely $\{3, 6, 7\}$. If e.g. the third edge on the inner rim were horizontal, the resulting skew diagram would be disconnected and therefore not a valid border strip, shown below.

(131)

It is clear that this holds generally for border strips. In particular, the inner and outer edges of any border strip are identical for $j = 2, 3, \dots, n$, and the outer (inner) edge for $j = 1$ is horizontal (vertical), whereas the outer (inner) edge for $j = n + 1$ is vertical (horizontal).

The configurations corresponding to λ and ν are related by taking the configuration on the outer rim of λ/ν (as a subset of the outer rim of λ) and replacing it by the configuration corresponding to the inner rim of λ/ν . What we effectively get is the following. We take a particle at some site k and move it to site $k - n$, and we get a factor $(-1)^{\text{ht}(\lambda/\nu)}$. Here, $\text{ht}(\lambda/\nu)$ equals the number of particles the affected particle jumps over, that is, the number of particles occupying sites $\{k - n + 1, \dots, k - 1\}$. We thus see that $(-1)^{\text{ht}(\lambda/\nu)}$ simply implements *fermionic statistics*. Below, we show the border strip λ/ν with empty cells

as a subset of λ , where we indicate particles and holes. The inner edge j and outer edge j for $j = 2, \dots, n$ are connected by diagonal lines.



The configurations corresponding to λ and ν are given by

$$\begin{aligned}
 |\lambda\rangle &= \dots \bullet \circ \bullet \circ \circ \circ \bullet \circ \circ \bullet \bullet \circ \circ \bullet \circ \dots, \\
 |\nu\rangle &= \dots \bullet \circ \bullet \circ \bullet \circ \bullet \circ \circ \bullet \bullet \circ \circ \circ \circ \dots.
 \end{aligned} \tag{133}$$

It is clear that they are identical except for a single particle which has moved $n = 9$ sites to the left, whereby it jumps over 3 other particles, leading to a factor $(-1)^3$. Summarizing the above, we have

$$\sum_{r=0}^{n-1} (-1)^r G_{\lambda; (n-r, 1^r)}^c = \sum (-1)^P s_{\lambda \setminus \eta}(y) \left\{ \begin{array}{l} \text{Distinct ways to move a particle in } \lambda \\ \text{to the left by } n \text{ sites, thereby hopping} \\ \text{over } P \leq n - 1 \text{ other particles.} \end{array} \right\}, \tag{134}$$

where $\lambda \setminus \eta$ again represents a diagram obtained from λ by the removal of a border strip, in this case of size n . We can apply the reasoning presented above to the calculation of $\chi_{\alpha}^{\lambda/\mu}$, by considering $p_{\alpha} s_{\mu}$ in terms of fermionic particles hopping on a 1D lattice. In particular, starting from some partition μ and fixing a choice of α , we consider all way to consecutively take a particle in the configuration corresponding to μ and move it α_j sites to the right, summing over $j \geq 1$, and adding a multiplicative factor -1 for each other particle which it hops over. We then add the resulting numbers (± 1) for all cases where the end result of this process is the configuration λ . The outcome of this computation is precisely $\chi_{\alpha}^{\lambda/\mu}$. This might provide a convenient method for computing $\chi_{\alpha}^{\lambda/\mu}$, as it involves moving particles around on a line instead of a border strip tiling problem. Although these two problems evidently identical, the former might be simpler to implement practically.

3.2.1 The action of the hamiltonian in terms of Young diagrams

When we consider the action of the hamiltonian in (225) in terms of diagrams, the following picture arises. The presentation given here does not depend on taking $N \rightarrow \infty$ and holds for finite N as well. We first consider the XX0-model, in which case the action of H^n on some state with k particles can be described in terms of k non-intersecting (vicious) random walkers that are allowed to take a single site to the left or

(138)

Consider a generalization of the Young's lattice in the form of a graph where each edge connects two diagrams that are related by addition or removal of some size n border strip, for all n . The action $H^n |\lambda\rangle$ of a general long-range hamiltonian as in (225) corresponds to an n -site random walk on this graph, where edges corresponding to a border strip of size n carry weight a_n . This provides a general description of the action of a hamiltonian in (225) in terms of (addition and removal of) border strips. We know from equation (215) how many diagrams there are with some n -core μ and n -weight w , but due to the fact that the graph described above has varying connectivity, the n -site random walk is more likely to end up in some diagrams than others.

3.2.2 Border strip tableaux and fermionic models

As in section 3.2.1, the present treatment up to equation (141) does not require $N \rightarrow \infty$. We saw that adding or removing a border strip η and multiplying with $(-1)^{\text{ht}(\eta)}$ implements fermionic statistics, and that this can be applied to the calculation of $\chi_\alpha^{\lambda/\mu}$. Inverting this line of reasoning, we will now derive two relations for fermionic models using the properties of $\chi_\alpha^{\lambda/\mu}$. The first of these involves the fact, noted at equation (202) and below, that the order in which one adds border strips in the construction of a border strip tableau $\text{BST}(\lambda/\mu, \alpha)$ is irrelevant to its outcome. That is, $\chi_\alpha^{\lambda/\mu}$ does not depend on the order of the entries of α . The same is true for the removal of border strips, as can be seen in equation (208) and the example in (210) and figure 2. From the relation between removing or adding border strips in the construction of $\chi_\alpha^{\lambda/\mu}$ and fermions hopping on a line, we can make the following observation. Consider a one-dimensional fermion configuration corresponding to some diagram μ , and consider all ways of moving not necessarily distinct fermions to the right by $\alpha_1, \alpha_2, \dots$ sites, where α_j are unordered non-negative integers. We then see that *the order of the step sizes α_j by which we move fermions has no effect on the outcome of this process*. That is, starting from a fermionic configuration and consecutively moving fermions to the right by various step sizes, the outcome depends only on the distribution of the step sizes and not the order in which the steps are taken. It is clear from applying (208) and the removal of border strips in the computation of $\chi_\alpha^{\lambda/\mu}$ that the same statement holds when we consider fermions that can only hop to the left instead of the right.

Consider a simple example which is partly given in figure 2 and in its entirety in figure 1. Namely, consider again $\lambda = (3, 2) =$

and now remove twice a single cell and once a border strip of size 2 from λ .

We can see this gives \square , regardless of the order of the border strip sizes.

$$\begin{array}{l}
\begin{array}{|c|c|c|} \hline \square & \square & \square \\ \hline \square & & \\ \hline \end{array} \xrightarrow{p_2} \begin{array}{|c|c|c|} \hline \square & \square & \square \\ \hline \square & & \\ \hline \end{array} \xrightarrow{p_1} \begin{array}{|c|c|} \hline \square & \square \\ \hline \square & \\ \hline \end{array} \xrightarrow{p_1} \square \\
\\
\begin{array}{|c|c|c|} \hline \square & \square & \square \\ \hline \square & & \\ \hline \end{array} \xrightarrow{p_1} \begin{array}{|c|c|c|} \hline \square & \square & \square \\ \hline \square & & \\ \hline \end{array} + \begin{array}{|c|c|} \hline \square & \square \\ \hline \square & \\ \hline \end{array} \xrightarrow{p_2} \begin{array}{|c|c|} \hline \square & \square \\ \hline \square & \\ \hline \end{array} + (1-1) \times \begin{array}{|c|} \hline \square \\ \hline \square \\ \hline \end{array} \xrightarrow{p_1} \square \\
\\
\begin{array}{|c|c|c|} \hline \square & \square & \square \\ \hline \square & & \\ \hline \end{array} \xrightarrow{p_1} \begin{array}{|c|c|c|} \hline \square & \square & \square \\ \hline \square & & \\ \hline \end{array} + \begin{array}{|c|c|} \hline \square & \square \\ \hline \square & \\ \hline \end{array} \xrightarrow{p_1} 2 \times \begin{array}{|c|c|} \hline \square & \square \\ \hline \square & \\ \hline \end{array} + \begin{array}{|c|c|c|} \hline \square & \square & \square \\ \hline \square & & \\ \hline \end{array} \xrightarrow{p_2} \square
\end{array} \tag{139}$$

It is interesting to see that the fact that we arrive at \square follows either from the cancellation between two different ways to arrive at $\begin{array}{|c|} \hline \square \\ \hline \square \\ \hline \end{array}$, in the second line of (139), or the fact that one cannot remove a size 2 border strip from $\begin{array}{|c|c|} \hline \square & \square \\ \hline \square & \\ \hline \end{array}$, in the third line of (139). Assigning particle-hole configurations to the diagrams above, given in (103) for $\begin{array}{|c|c|c|} \hline \square & \square & \square \\ \hline \square & & \\ \hline \end{array}$, and treating the particles as fermions gives an example of the irrelevance of the order of step sizes.

Our second result for fermionic systems arises from equations (213), (214). These state that $\chi_{(n^k)}^{\lambda/\mu}$ is cancellation-free, where μ is the n -core of λ [42], [41]. This leads to the following observation. Take a fermionic hamiltonian \hat{H}_f , where fermions are only allowed to hop n sites, and denote a fermionic state corresponding to the n -core μ of some λ as $\|\mu\rangle\rangle$. The result of $\hat{H}_f\|\mu\rangle\rangle$ can then be expressed in terms of symmetric functions as

$$s_\mu D_n + \sum_{r=0}^{n-1} (-1)^r s_{\mu/(n-r,1^r)} = \sum_{\nu} (-1)^{\text{ht}(\nu/\mu)} s_\nu + \sum_{\nu_n} (-1)^{\text{ht}(\eta)} s_{\mu \setminus \eta}, \tag{140}$$

where, as before, ν and $\mu \setminus \eta$ are related to μ by the addition and removal of a border strip of size n , respectively. Compare with equation (135), especially the factors $(-1)^{\text{ht}}$. We can keep iterating this step by adding and removing border strips of size n to and from the resulting diagrams. From (213) and the comments below, it then follows that all diagrams appearing in the expansion of $(\hat{H}_f)^k \|\mu\rangle\rangle$ have the same sign *for any* k . Further, we saw that adding or removing border strips μ/ν and multiplying by $(-1)^{\text{ht}(\mu/\nu)}$ corresponds to letting fermions hop over a distance of $|\mu/\nu|$ lattice sites. It follows that, for a fermionic model where particles can only hop n sites, *all distinct ways to go from some configuration μ to another configuration λ appear with the same sign, with the sign depending only on the choice of μ and λ* . In other words, all different ways to go from any configuration μ to any other configuration λ involves fermions hopping over either an even or an odd number of other fermions. Physically, this means that there is no interference between various ways to arrive at some fermionic state. Fermionic states will spread through Hilbert space rapidly upon time evolution, as they are not restricted by destructive interference.

The same reasoning can be applied to various expectation values of the LRRW models with hamiltonian (225). In particular, we will consider $\langle\langle \text{tr} U^n \rangle\rangle_c$. Repeatedly applying (197), which we have

used at various points above, we get

$$\langle (\text{tr} U^n)^k s_\lambda(U^{-1}) \rangle_c = \sum_{j=1}^k \sum_{\nu_{n,j}} (-1)^{\text{ht}(T_j)} s_{\nu_{n,j}}(x) p_n(y)^{k-j} . \quad (141)$$

where we use the notation $\nu_{n,j}$ for diagrams related to λ by the consecutive removal of j border strips of size n . For example, consider again $\lambda = (6, 5, 2^2, 1)$ and $(n^k) = (4^4)$. Then, the diagrams $\nu_{4,2}$ are given by removing the yellow and blue regions from the diagrams in (216), for $\nu_{4,3}$ the orange regions are also removed, and after removing the red regions we end up with $\nu_{4,4} = \emptyset$. Note that $\chi_{(n^k)}^\lambda = 0$ for most λ , one sufficient but far from necessary condition for this being that $nk \neq |\lambda|$. In general, consecutively removing border strips of some size n leads eventually to the aforementioned n -core of λ [44]. From (119), we have

$$s_{\nu_{n,j}}(x) p_n^{k-j}(x) = \sum_{\mu} d_{n,j,k}^{\mu} s_{\mu}(x) , \quad (142)$$

for some coefficients $d_{n,j,k}^{\mu}$. From (195), we know that $s_{\lambda} p_n^k$ is expanded as a sum over all diagrams related to λ by subsequently adding a k border strips of size n . On the other hand, $\nu_{n,j}$ is related to λ by removal of j border strips of size j . Therefore,

$$\langle (\text{tr} U^n)^k s_{\lambda}(U^{-1}) \rangle_c = \sum_{j=1}^k \sum_{\tilde{\nu}_{n,j}^k} e^{i\phi(k-j)} (-1)^{\text{ht}(T_1) + \text{ht}(T_2)} s_{\tilde{\nu}_{n,j}^{k-j}}(x) . \quad (143)$$

In the above expression, the sum is over all $\tilde{\nu}_{n,j}^{k-j}$ constructed by first removing j border strips of size n from λ (which results in $\nu_{n,j}$) and then adding $k - j$ border strips of size n , including multiplicities. Further, T_1 is given by the BST constructed from of the union of the j border strips that are removed from λ , and T_2 is the tableau that is the union of the $k - j$ border strips that are added to $\nu_{n,j}$ to construct $\tilde{\nu}_{n,j}^{k-j}$. For $\lambda = (6, 5, 2^2, 1)$, we consider

$$\langle (\text{tr} U^4)^2 s_{\lambda}(U^{-1}) \rangle_c . \quad (144)$$

As mentioned above, contracting both copies of $\text{tr} U^4$ with s_{λ} gives rise to the diagrams in (216) after removing the yellow and blue border strips. The $\tilde{\nu}_{4,1}^1$ are given by the ways to remove from and then add to λ a border strip of size four. We see from (143) that λ appears in the expansion of (144) with a multiplicity two, as there are two distinct border strips of size four that one can remove from λ , namely, the yellow and blue border strips on the leftmost diagram in (216). To find the remaining diagrams appearing in (144), one should add border strips of size four to the diagrams obtained after removing the yellow and

blue border strips on the leftmost diagram in (216). In general, we get the following picture.

$$\langle (\text{tr} U^n)^k s_\lambda(U^{-1}) \rangle_c = \pm \sum_{j=1}^k e^{i\phi(k-j)} s_{\nu_{n,j}^{k-j}}(x) \left\{ \begin{array}{l} \text{Distinct ways to consecutively} \\ \text{move } j \text{ particles in } \lambda \text{ to the left} \\ \text{by } n \text{ sites and then move } k-j \\ \text{particles to the right by } n \text{ sites .} \end{array} \right\} \quad (145)$$

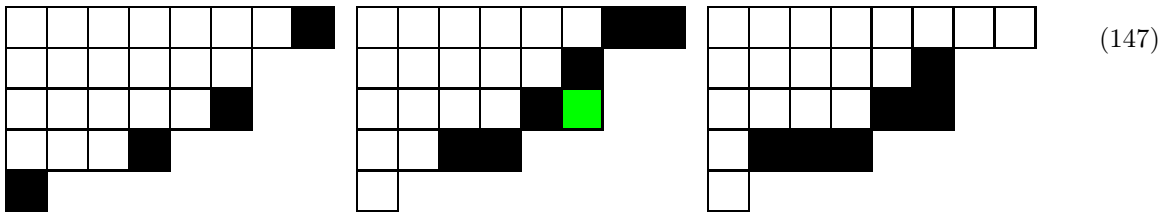
Note that the particles that are moved by n sites are not necessarily distinct. Further, the right hand side appears with a positive or negative sign depending only on the final configuration. This again follows from the fact that $\chi_\alpha^{\lambda/\mu}$ is cancellation-free.

3.2.3 Schur polynomial expansions of correlation functions

We consider now the expansions for general correlation functions which were derived in section 2.3. We first consider the application of (52) here, before moving on to (68) in section 3.2.4. Equation (52) expresses $\langle s_\lambda(U) s_\nu(U^{-1}) \rangle$ as a sum over diagrams obtained from λ and ν by removing border strips of size $\alpha_1, \alpha_2, \dots$ for a composition α , summed over α up to permutations of the entries α_j . In particular, it establishes a relation between $\langle s_\lambda s_\nu \rangle_c$ and the correlation functions $\langle s_{\lambda \setminus \{\eta\}} \rangle = \langle \emptyset | s_{\lambda \setminus \{\eta\}} \rangle$, involving only a single non-trivial configuration $\lambda \setminus \{\eta\}$ (and likewise for $\nu \setminus \{\eta\}$). Fixing some α , we sum over all ways to start from λ and ν and move particles α_j sites to the left with fermionic statistics (in the form of $(-1)^{\text{ht}(T_\eta)}$). Consider the autocorrelation for $\nu = \lambda = (8, 6^2, 4, 1)$, which we show below.



Equation (52) gives an expression in terms of diagrams obtained by removing border strips from λ . Below, we show from left to right all border strips of size 1, 2, 3 that can be removed from $\lambda = \nu$.



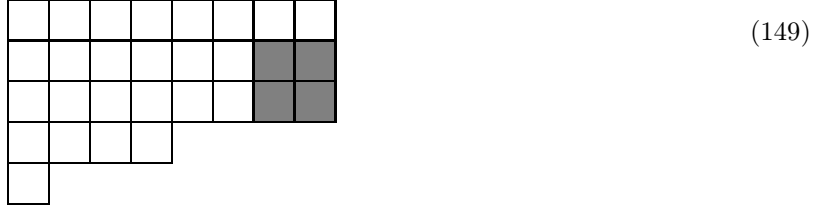
In the middle diagram above, the green cell is shared between both a horizontal and a vertical strip of size two. We can thus remove four border strips of both size 1 and 2, and two of size 3. It is easy to see that there is a single border strip of size 4 that can be removed from λ , three border strips for both sizes 5 and

6, and so on, up to a single border strip of size $\lambda_1 + \ell(\lambda) - 1 = 12$. Applying (52) then gives

$$\begin{aligned} \langle s_\lambda(U)s_\lambda(U^{-1}) \rangle_c &= (s_{(7,6^2,4,1)} + s_{(8,6,5,4,1)} + s_{(8,6^2,3,1)} + s_{(8,6^2,4)})^2 + \\ &+ \frac{1}{2} (s_{(6^3,4,1)} - s_{(8,5^2,4,1)} + s_{(8,6,4^2,1)})^2 + \frac{1}{3} (-s_{(8,5,4,1^2)} + s_{(8,6^2,1^2)})^2 + \dots \end{aligned} \quad (148)$$

In the above expression, the first, second, and third terms correspond to the removal of border strips of size one, two, and three, respectively. Further, we again write $(s_\mu + s_\rho + \dots)^2$ instead of $(s_\mu(x) + s_\rho(x) + \dots)(s_\mu(y) + s_\rho(y) + \dots)$.

Consider now $\langle s_\lambda(U)s_\nu(U^{-1}) \rangle$ with λ as above and $\nu = (8^3, 4, 1)$, the latter of which is shown below. We have here $\lambda \subset \nu$, and we indicate ν/λ in gray.



Consider again all ways to remove border strips from ν , and apply (52). This then leads to the following terms appearing in the expansion of $\langle s_\lambda(U)s_\nu(U^{-1}) \rangle$,

$$\begin{aligned} &(s_{(7,6^2,4,1)} + s_{(8,6,5,4,1)} + s_{(8,6^2,3,1)} + s_{(8,6^2,4)}) (s_{(8^2,7,4,1)} + s_{(8^3,3,1)} + s_{(8^3,4)}) + \\ &+ \frac{1}{2} (s_{(6^3,4,1)} - s_{(8,5^2,4,1)} + s_{(8,6,4^2,1)}) (s_{(8,7^2,4,1)} + s_{(8^2,6,4,1)} + s_{(8^3,2,1)}) + \dots \end{aligned} \quad (150)$$

The diagrams appearing on the left (right) in the top and bottom lines of (150) are found by removing border strips of sizes 1 and 2 from λ (ν), respectively. This expansion can easily be continued by considering more or larger border strips. From the relation between removal or addition of border strips as in (52) and fermionic particles hopping on a line, we can interpret (52) in the following manner.

$$\langle s_\lambda s_\nu \rangle = \sum_\alpha \frac{1}{z_\alpha} \left((-1)^P s_{\lambda \setminus \{\eta\}}(y) \left\{ \begin{array}{l} \text{Distinct ways to take particles in } \lambda \\ \text{and move them } \alpha_1, \alpha_2, \dots \text{ sites to the} \\ \text{left, thereby hopping over } P \text{ particles} \end{array} \right\} \times \binom{y \rightarrow x}{\lambda \rightarrow \nu} \right) \quad (151)$$

We remind the reader that $\{\eta\} = \{\eta_1, \eta_2, \dots\}$ are border strips of sizes $|\eta_j| = \alpha_j$. Note that the particles mentioned above are not required to be distinct.

3.2.4 Power sum expansions of correlation functions

From the fact that, for $\tau = it$, $p_k(x)$ and $p_k(y)$ are related by a phase, it is useful to express LRRW correlation functions as expansions in terms of $p_k(x)$ and $p_k(y)$ in order to reveal these phases. To do so, one may use the relation between Schur and power sum polynomials in equation (201) and apply the Murnaghan-Nakayama rule, as done for the relatively simple example of $\langle s_\lambda(U)s_\lambda(U^{-1}) \rangle$ for $\lambda = (3, 2)$ in

section 2.3.2. However, as noted there, even this relatively simple example is already somewhat non-trivial, as it requires the computation of χ^λ_α for all α . For these purposes, it is more convenient to employ (68), which provides an expansion of $\langle s_\lambda(U)s_\nu(U^{-1}) \rangle$ in terms of $p_k(x)$ and $p_k(y)$. The prefactors appearing in this expansion depend on the number of ways to remove border strips from λ and ν in such a way that the resulting diagram is the same for both λ and ν . Taking again $\nu = \lambda = (8, 6^2, 4, 1)$, for which the diagrams resulting from removal of border strips were treated in section 3.2.3 above. Applying (68) then gives

$$\begin{aligned} \langle s_\lambda(U)s_\lambda(U^{-1}) \rangle_c &= 4p_1(x)p_1(y) + p_2(x)p_2(y) + \frac{2}{9}p_3(x)p_3(y) + \frac{1}{16}p_4(x)p_4(y) + \\ &+ 3 \left(\frac{1}{25}p_5(x)p_5(y) + \frac{1}{36}p_6(x)p_6(y) \right) + \\ &+ \frac{1}{2} (p_1^2(x)p_2(y) + p_2(x)p_1^2(y)) + \\ &+ \frac{1}{6} (p_3(x)p_1(y)p_2(y) + p_3(y)p_1(x)p_2(x)) + \dots \end{aligned} \quad (152)$$

In the above expression, the first two lines on the right hand side are given by (62), which is a special case of (68). As we saw previously, the terms $\sim \frac{p_i(x)p_j(y)}{j^2}$ in the first two lines of (152) arise as follows. The denominator is given by the inverse of $z_{(j)}z_{(j)} = j^2$, and the numerator equals the number of distinct ways to remove a border strip of size j from $\lambda = (3, 2)$. The third and fourth line give mixed power sums obtained from not contracting a single $p_j(U^\pm)$ and two copies of $p_k(U^\mp)$, $p_m(U^\mp)$. From the diagrams in (147), one can see that there are four ways to remove two border strips of unit size and arrive at a diagram that can alternatively be obtained by removing a single border strip of size 2. This follows from the fact that there are four ways to remove a border strip of size two, which can alternatively be achieved by removing the two cells of such a border strip successively. However, due to the factors $(-1)^{\text{ht}(T)}$ in (68), one of those four contributes with a negative sign, leading to a prefactor of $\frac{2}{z_{(1^2)}z_{(2)}} = \frac{1}{2}$ multiplying $\sim p_1^2 p_2$ in the third line of (152). There is a similar cancellation occurring from the term proportional to $p_3 p_1 p_2$. This expansion can then be continued by removing further border strips. Consider again $\langle s_\lambda(U)s_\nu(U^{-1}) \rangle$ with $\lambda = (8, 6^2, 4, 1)$ and $\nu = (8^3, 4, 1)$, as at the end of section 3.2.3. applying (68) leads to

$$\langle s_\lambda(U)s_\nu(U^{-1}) \rangle = -\frac{2}{3}p_1(x)p_3(x) + \frac{1}{4}p_2^2(x) + \frac{1}{12}p_1(x)^4 + \frac{1}{2}p_2^2(x)p_1(x)p_1(y) + \dots \quad (153)$$

This can be seen by considering diagram corresponding to ν in (149), and covering the gray 2 by 2 square with border strips of sizes from 1 to 3. We get no contribution proportional to $p_2(x)p_1(x)^2$ since the two ways to cover a 2 by 2 diagram with a single border strip of size 2 and 2 border strips of size 1 appear with opposite sign. This expansion can be continued by removing more or larger border strips from λ and ν , which can be conveniently done by using the relation to fermionic configurations.

The above examples show that (68) can be conveniently applied to $\langle s_\lambda(U)s_\nu(U^{-1}) \rangle$ for larger λ, ν as well, for which χ^λ_α and χ^ν_α would be very hard to compute. Indeed, as hinted at above, it is particularly useful for the following three reasons.

1. Equation (68) provides a controlled expansion of general correlation functions $\langle s_\lambda(U)s_\nu(U^{-1}) \rangle$ in terms of power sums. These power sums can be directly read off from the hamiltonian, see (88) and

(90).

2. This expansion can be straightforwardly applied, including to correlation functions involving large diagrams λ, ν . Using the comments below (128), the removal of border strips is related to fermionic particles hopping on a line, which could further simplify the application of this method.
3. The power sums $p_k(x)$ and $p_k(y)$ are proportional to τ , so that (68) provides an expansion in terms of powers of τ . Depending on the application and the range of τ one would like to consider, this expansion can be truncated at any desirable order that provides sufficient precision. For $\tau = it$, this $p_k(x)$ and $p_k(y)$ are related by a complex phase, leading to various simplifications that are hard to reveal otherwise.

From the treatment above, it follows that the expression for $\langle s_\lambda(U)s_\nu(U^{-1}) \rangle$ in equation (68) has the following particle-hole interpretation.

$$\langle s_\lambda(U)s_\nu(U^{-1}) \rangle = \sum_{\omega, \gamma} \frac{p_\omega(y)p_\gamma(x)}{z_\omega z_\gamma} (-1)^P \left\{ \begin{array}{l} \text{Distinct ways to move particles in } \lambda \text{ and } \nu \\ \text{to the left by } \gamma_1, \gamma_2, \dots \text{ and } \omega_1, \omega_2, \dots \text{ sites,} \\ \text{respectively, hopping over } P \text{ other particles} \\ \text{and ending up in the same configuration.} \end{array} \right\} \quad (154)$$

3.2.5 Correlations for power sums and applications to experimental benchmarking

We give here some suggestions for the benchmarking of experimental setups using correlation functions involving power sum polynomials. In experimental contexts such as trapped ion systems, one could measure the correlation functions corresponding to $\langle p_n(U^{\pm 1}) \rangle = \langle \text{tr} U^{\pm n} \rangle = p_n$ experimentally. Remember that p_n can be read off from the hamiltonian as in (88) or (90) due to their direct proportionality to $a_{\pm n}$, and is given by a superposition of configurations corresponding to hook-shaped diagrams as in (121). Therefore, one could measure $\langle p_n(U^{\pm 1}) \rangle$ and compare them with the intended values of $a_{\pm n}$ to benchmark experimental setups. Further, one can use equation (7),

$$\langle |\text{tr} U^n|^2 \rangle = n + p_n(x)p_n(y), \quad (155)$$

and consider $\text{tr} U^n$ as a superposition of states (when properly normalized), as before. Then, the correlation function corresponding $\langle |\text{tr} U^n|^2 \rangle$ is proportional to $F_{\emptyset; \emptyset}$ with proportionality given by $n + p_n(x)p_n(y)$, up to normalization. When we have certain hopping parameters $a_n \neq 0$, the only way to get independence from time is to have no dependence on the power sums $p_n \sim \tau n a_n$, as they contain a factor of τ . The τ -independence of the connected part of the correlation function corresponding to (7) therefore sets it apart from other correlation functions, and might offer an effective way to benchmark experimental setups. Remember that the p_λ form a basis for all symmetric polynomials. In case $\ell(\lambda) \geq 2$ (or $\ell(\nu) \geq 2$) so that $p_\lambda = p_{\lambda_1} p_{\lambda_2} \dots$, Wick's theorem tells us that $\langle p_\lambda p_\mu \rangle_c$ will contain terms where not all p_{λ_j} and p_{μ_k} are contracted. These give contributions containing $p_k(x) \sim \tau$ (and/or $p_j(y) \sim \tau$). Therefore, $\frac{1}{\sqrt{n}} \langle |\text{tr} U^n|^2 \rangle_c$ for any integer n is the only non-zero connected correlation function that does not depend on τ . Lastly, one could use $\langle \text{tr} U^n \text{tr} U^{-k} \rangle_c = n \delta_{n,k}$ (after proper normalization) to see if the system is truly translationally

invariant, as its derivation is predicated on the assumption of translational invariance.

4 Conclusions

This work focused on weighted $U(N)$ integrals over symmetric polynomials and their relation with correlation functions of LRRW models. The weighting is given by a weight function $f(z)$, which is required to satisfy Szegő's strong limit theorem, corresponding to hopping parameters a_k whose modulus decays faster than k^{-1} for $k \rightarrow \infty$. Writing the weight function in terms of generating functions of elementary or complete homogeneous symmetric polynomials as $f(z) = E(x; z)E(y; z^{-1})$ or $f(z) = H(x; z)H(y; z^{-1})$, respectively, general correlation functions can be expressed in terms of Schur polynomials with variables x and y . In particular, the power sum polynomials are related to the hopping parameters as $p_k(x) = \pm \tau k a_k$ and $p_k(y) = \pm \tau k a_{-k}$ for $k \geq 1$. By using our earlier result [40] that $\langle \text{tr} U^n \text{tr} U^{-k} \rangle_c = n \delta_{n,k}$ and applying Wick's theorem, we derive various identities. In particular, we compute $\langle p_\mu(U) p_\rho(U^{-1}) \rangle$, generalizing a result due to Diaconis and Shahshahani, who computed said object in the CUE, corresponding to $f = 1$. Further, we derive two expressions for correlation functions $\langle s_\lambda(U) s_\nu(U^{-1}) \rangle$ for general λ and ν , both of which are obtained by removing border strips from λ and ν . In particular, the first of these expressions is an expansion in terms of diagrams related to λ and ν by the removal of border strips. The second is an expansion in terms of $p_\gamma(x)$ and $p_\omega(y)$, where the expansion coefficients are determined by the number of ways to remove border strips from λ and ν and arrive at the same diagram, up to a sign determined by the height of the (generally disjoint) border strip tableau that is removed.

We applied these results to correlation functions of LRRW models, where we consider configurations starting with an infinite number of particles (down spins) and ending with an infinite number of holes (up spins). Before applying our own results, we considered various standard relations in the theory of symmetric polynomials, such as the Pieri formula, which lead to a simple way to compute and interpret various correlation functions. The most striking of these results is the fact that the involution between elementary and complete homogeneous symmetric polynomials, corresponding to the transposition of diagrams, leads to a duality between models related by switching the sign of the even hopping parameters, $a_k \rightarrow (-1)^{k+1} a_k$. In particular, we found that the correlation functions of these two models equal each other when we perform a particle-hole and parity transformation, which acts non-trivially on the finite interval in between the infinite strings of particles and holes. We therefore refer to this duality as quasi-local particle-hole duality. Further, we noted that the Jacobi-Trudi identity allows one to calculate any $\langle s_\lambda(U) s_\nu(U^{-1}) \rangle$ directly. Although the number of terms appearing in this expansion grows quickly with the size of λ, ν , it is simple to implement as it only involves the calculation of a determinant of a matrix with known entries.

We then considered the basis of power sum polynomials $p_\gamma(x)$ and $p_\omega(y)$ and the closely related border strips, which is particularly useful in the application to LRRW models due to their aforementioned relation to hopping parameters a_k and generalized time τ . As mentioned above, we derived expressions for LRRW correlation functions involving addition or removal of a border strip T of size n and height $\text{ht}(T)$, leading to a sign $(-1)^{\text{ht}(T)}$. We found that this corresponds to moving a fermionic particle a distance n to the right or left, respectively, thereby hopping over $\text{ht}(T)$ other particles. This provides an interpretation of various

expansions of correlation functions in terms of particles hopping with fermionic exchange statistics, even though the LRRW model consists of hard-core bosons rather than fermions. For example, the procedure of the second expansion of $\langle s_\lambda s_\nu \rangle$, in (68), which involves the removal of border strips, can be interpreted as replacing the (hard-core boson) particles in λ and ν by fermions and considering all distinct ways to move them to the left such that the final configurations are identical. Due to the aforementioned relation between power sums and hopping parameters, this expression provides an expansion in powers of τ where the numbers appearing in the expansion coefficients can be read off from the hamiltonian.

The mathematical results derived in section 2 may be generally applied to the case where the strong Szegő limit theorem applies. The expansion of general correlation functions in terms of power sum polynomials is particularly useful in such applications where these can be accessed directly, such as for LRRW models, where they are provided as input. In section 3, we saw that the addition or removal of border strips with sign $(-1)^{\text{ht}}$ can be interpreted as fermionic particles hopping to the right or left, respectively. One may apply this ‘physical’ interpretation of this process to the power sum expansion of $\langle s_\lambda s_\nu \rangle$, by considering all ways to move fermionic particles in λ and ν to the left to arrive at the same configuration. Further, the same fermionic interpretation may be applied to the Murnaghan-Nakayama rule, which could provide a more convenient practical method for the calculation of general $\chi_\alpha^{\lambda/\mu}$. Inverting this reasoning, we applied properties of these character to long-range fermionic models. First of all, the fact that $\chi_\alpha^{\lambda/\mu}$ does not depend on the order of the entries of α , means that taking a fermionic configuration and considering all ways to move particles by $\alpha_1, \alpha_2, \dots$ sites to the right gives the same outcome regardless of the ordering of the step sizes α_j . Further, the fact that the symmetric group character are cancellation-free for $\alpha = (n^k)$ lead to the conclusion that all ways to go from any configuration to any other configuration by taking only n sites involves either an even or an odd number of particles being hopped over, depending only on n and the choice of initial and final configurations.

As mentioned in the introduction, LRRW models such as we consider here have seen increasing activity in both experimental and theoretical contexts due to the experimental accessibility of such systems and the surprising phenomena they exhibit. We believe our work can be applied along some of these lines of research, including the consideration of localization by addition of (diagonal) disorder [29], [30]. Adding such disorder will generally break translational invariance, and the expressions in this work will no longer apply. One may also consider translationally invariant disorder such as random hopping parameters, as in [48], [49], in which case the results derived here would still apply as long as the hopping parameters satisfy the aforementioned asymptotic fall-off conditions. All results in section 3 can, in principle, be checked experimentally, where the expressions in this work would be expected to hold with reasonable accuracy up to the time that finite size effects start to occur. Besides checking our results in experimental setups, correlation functions involving power sum polynomials may be used for experimental benchmarking.

5 Acknowledgements

We would like to thank Ivan Khaymovich, Vladimir Kravtsov, Jiří Minář, and Arghavan Safavi-Naini for useful discussions and suggestions. This work is part of the DeltaITP consortium, a program of the

Netherlands Organization for Scientific Research (NWO) funded by the Dutch Ministry of Education, Culture and Science (OCW).

Appendices

A Symmetric polynomials and Young diagrams

We review here some aspects of symmetric polynomials and Young diagrams, starting with some simple examples. Take a set of variables $x = (x_1, x_2, \dots)$. The *elementary symmetric polynomials* are then defined as

$$e_k(x) = \sum_{i_1 < \dots < i_k} x_{i_1} \dots x_{i_k} . \quad (156)$$

Some examples include

$$\begin{aligned} e_0 &= 1 , \\ e_1(x_1) &= x_1 , \\ e_1(x_1, x_2) &= x_1 + x_2 , \\ e_2(x_1, x_2) &= x_1 x_2 . \end{aligned} \quad (157)$$

Closely related are the *complete homogeneous symmetric polynomials*, defined as

$$h_k(x) = \sum_{i_1 \leq \dots \leq i_k} x_{i_1} \dots x_{i_k} , \quad (158)$$

which contain all monomials of degree k . Note the difference in the summation bounds between (156) and (158). Some examples of h_k include

$$\begin{aligned} h_0 &= 1 , \\ h_1(x_1) &= x_1 , \\ h_1(x_1, x_2) &= x_1 + x_2 , \\ h_2(x_1, x_2) &= x_1 x_2 + x_1^2 + x_2^2 . \end{aligned} \quad (159)$$

Another type of symmetric polynomial is the *power sum symmetric polynomial*, also simply referred to as *power sum polynomial*,

$$p_k(x) = \sum_j x_j^k = x_1^k + x_2^k + \dots \quad (160)$$

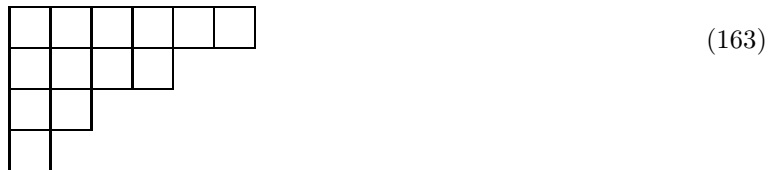
The generating functions of e_k and h_k and their relation with power sums are as follows [see e.g [50]],

$$\begin{aligned} E(x; z) &= \sum_{k=0}^{\infty} e_k(x) z^k = \prod_{k=1}^{\infty} (1 + x_k z) = \exp \left[\sum_{k=1}^{\infty} \frac{(-1)^{k+1}}{k} p_k(x) z^k \right], \\ H(x; z) &= \sum_{k=0}^{\infty} h_k(x) z^k = \prod_{k=1}^{\infty} \frac{1}{1 - x_k z} = \exp \left[\sum_{k=1}^{\infty} \frac{1}{k} p_k(x) z^k \right]. \end{aligned} \quad (161)$$

From the above expressions, it is clear that $H(x; z)E(x; -z) = 1$. Checking every order of z then gives, for all $n \geq 1$ and any choice of x [e.g. (2.6') from [50]],

$$\sum_{r=0}^n (-1)^r h_{n-r}(x) e_r(x) = 0. \quad (162)$$

Partitions play an important role in the study of symmetric polynomials. A partition of $n \in \mathbb{Z}^+$ is a sequence of non-negative integers $\lambda = (\lambda_1, \lambda_2, \dots, \lambda_{\ell(\lambda)})$, which we will order as $\lambda_1 \geq \lambda_2 \geq \dots$, satisfying $\sum_j \lambda_j = n$. The *size* (or *weight*) of a partition is given by the sum of its terms $|\lambda| = \sum_j \lambda_j$ and its *length* $\ell(\lambda)$ is the largest value of j such that $\lambda_j \neq 0$. Closely related to partitions of n are *compositions* of n , consisting also of a sequence of non-negative integers which sum to n , but where a different ordering in these integers defines a different composition. A *weak composition* of n is a composition which may include zeroes as its entries, that is, a set of non-negative integers which sum up to n . A partition of n corresponds to a Young (or Ferrers) diagram containing n cells, or 'boxes'. We will use these terms interchangeably. As an example, the diagram corresponding to a partition of 12 given by $\lambda = (6, 4, 2, 1)$ is given below, where λ_j equals the number of cells in the j^{th} row.



We will denote a diagram consisting of b rows of a cells by (a^b) . For a partition λ , we will write

$$e_\lambda = \prod_{j \geq 1} e_{\lambda_j}, \quad h_\lambda = \prod_{j \geq 1} h_{\lambda_j}, \quad p_\lambda = \prod_{j \geq 1} p_{\lambda_j}. \quad (164)$$

Further, we write

$$z_\lambda = \prod_{j \geq 1} j^{m_j} m_j!, \quad m_j(\lambda) = \text{Card}\{k : \lambda_k = j\}, \quad (165)$$

i.e. $m_j(\lambda)$ is the number of rows in λ of length j . We also write $\varepsilon_\lambda = (-1)^{|\lambda| - \ell(\lambda)}$. Newton's identities then read

$$\begin{aligned} h_n &= \sum_{|\lambda|=n} z_\lambda^{-1} p_\lambda , \\ e_n &= \sum_{|\lambda|=n} \varepsilon_\lambda z_\lambda^{-1} p_\lambda . \end{aligned} \tag{166}$$

In terms of the complete exponential Bell polynomial B_n ², we have

$$\begin{aligned} h_n &= \frac{1}{n!} B_n(p_1, p_2, 2!p_3, \dots, (n-1)!p_n) , \\ e_n &= \frac{(-1)^n}{n!} B_n(-p_1, -p_2, -2!p_3, \dots, -(n-1)!p_n) . \end{aligned} \tag{167}$$

Another type of symmetric polynomial is the *Schur polynomial*. Schur polynomials play an important role as characters of irreducible representations of general linear groups and subgroups thereof. Schur polynomials are associated to a partition λ and a set of variables $x = (x_1, x_2, \dots)$ in the following way. For a choice of λ , a *semistandard Young tableau* (SSYT) is given by positive integers $T_{i,j}$ satisfying $1 \leq i \leq \ell(\lambda)$ and $1 \leq j \leq \lambda_i$. These integers are required to increase weakly along every row and increase strongly along every column, i.e. $T_{i,j} \geq T_{i,j+1}$ and $T_{i,j} > T_{i+1,j}$ for all i, j . Label by α_i the number of times that the number i appears in the SSYT. We then define

$$x^T = x_1^{\alpha_1} x_2^{\alpha_2} \dots \tag{168}$$

The *Schur polynomial* $s_\lambda(x)$ is given by [44].

$$s_\lambda(x) = \sum_T x^T , \tag{169}$$

where the sum runs over all SSYT's corresponding to λ i.e. all possible ways to inscribe the diagram corresponding to λ with positive integers that increase weakly along rows and strictly along columns. If $\lambda_j = 0$ for all j , then λ is the empty partition, which we denote by $\lambda = \emptyset$. The Schur polynomial of the empty partition is set to unity, i.e.

$$s_{\emptyset}(x) = 1 , \tag{170}$$

which is independent of the choice of variables x . We give an example of an SSYT corresponding to a Young diagram $\lambda = (3, 2)$ and with non-zero variables x_1, x_2, x_3 .

$$\begin{array}{|c|c|c|} \hline 1 & 1 & 3 \\ \hline 2 & 3 & \\ \hline \end{array} , \tag{171}$$

²Complete Bell polynomials $B_n(x_1 \dots x_n)$ can be defined by their generating function, $\sum_{n=0}^{\infty} B_n(x_1 \dots x_n) t^n / n! = \exp(\sum_{j=1}^{\infty} x_j t^j / j!)$

From (180) one can see that the contribution of this SSYT is given by $x_1^2 x_2 x_3^2$. Summing over all monomials corresponding to all SSYT's then gives the Schur polynomial $s_{(3,2)}(x_1, x_2, x_3)$. We emphasize that the result is generally a symmetric polynomial, as this may not be obvious from the definition. Consider the Schur polynomials corresponding to a row or a column of n cells, shown below for $n = 4$.

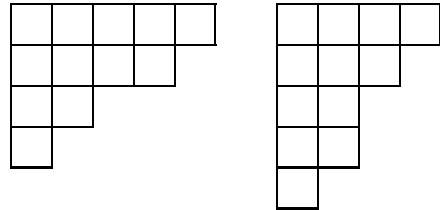


(172)

One can see that

$$s_{(1^n)} = e_n \quad , \quad s_{(n)} = h_n \quad , \quad (173)$$

for any choice of x . That is, the Schur polynomial of a column or row of n cells is given by the degree n elementary or complete homogeneous symmetric polynomial, respectively. Equation (173) simply follows from the requirement for SSYT's that integers increase weakly along rows and strongly along columns, compare with (156) and (158). It follows that we can exchange between e_n and h_n by transposing diagrams, that is, by reflecting across the main diagonal of the diagram, as this exchanges rows and columns. For a diagram λ , its transpose is denoted as λ^t . Since transposition is a reflection, it is an involution, i.e. $(\lambda^t)^t = \lambda$. It is clear that $(n)^t = (1^n)$ i.e. this involution maps rows to columns and vice versa. As a less trivial example, take $\lambda = (5, 4, 2, 1)$, shown below on the left, and $\lambda^t = (4, 3, 2^2, 1)$, shown on the right.



(174)

Power sum polynomials can also be expressed in terms of Schur polynomials, in this case in the form of a sum,

$$p_n = \sum_{r=0}^{n-1} (-1)^r s_{(n-r, 1^r)} \quad . \quad (175)$$

Here, $(a, 1^b)$ is a hook-shaped diagram consisting of a row with a cells followed by b rows with a single cell. For example, $\lambda = (5, 1^3)$ is given by the following diagram.



(176)

Although equation (175) may not be immediately obvious, it can easily be seen to arise in simple examples. If $x = (x_1, x_2)$ and $n = 1$, we have the following SSYT's.

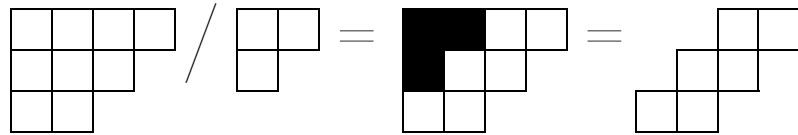
$$\boxed{1} + \boxed{2} \tag{177}$$

Which gives $p_1(x) = s_{(1)}(x_1, x_2) = x_1 + x_2$. For $n = 2$, the following SSYT's contribute,

$$\boxed{1} \boxed{1} + \boxed{1} \boxed{2} + \boxed{2} \boxed{2} - \begin{array}{|c|} \hline 1 \\ \hline 2 \\ \hline \end{array} \tag{178}$$

Note that the rightmost SSYT corresponding to (1^2) contributes with a minus sign, which results in $p_2(x) = s_{(2)}(x_1, x_2) - s_{(1^2)}(x_1, x_2) = x_1^2 + x_2^2$. One may convince oneself that this generalizes to higher n and general choice of x .

Schur polynomials have a natural generalization to so-called *skew Schur polynomials*, which are associated to skew diagrams. Skew diagrams are constructed from two non-skew diagrams λ and μ such that $\mu \subseteq \lambda$, which means that $\mu_i \leq \lambda_i, \forall i$. The skew diagram denoted by λ/μ is then the complement of μ in the diagram corresponding to λ . For $\lambda = (4, 3, 2)$ and $\mu = (2, 1)$, the skew diagram λ/μ is given by the following, where we indicate in black those cells which are removed from λ .



$$\tag{179}$$

The skew diagram on the right hand side is a *border strip*, which is a connected skew diagram not containing a 2 by 2 subdiagram. This is an important class of skew diagrams which we will encounter again later. For a general skew diagram, define a skew semistandard Young tableau corresponding to λ/μ as above, namely, as an array of positive integers T_{ij} satisfying $1 \leq i \leq \ell(\lambda)$ and $\mu_i \leq j \leq \lambda_i$ which increase weakly along rows and strictly along columns. We then define the *skew Schur polynomial* corresponding to λ/μ as

$$s_{\lambda/\mu} = \sum_T x^T, \tag{180}$$

where the sum again runs over all SSYT's corresponding to λ/μ . Note that if $\mu = \emptyset$, we have $s_{\lambda/\mu} = s_\lambda$, and if $\mu = \lambda$, $s_{\lambda/\lambda} = s_\emptyset = 1$. Let us consider $\lambda = (3, 2)$ and $\mu = (1)$. Below, we give a skew SSYT corresponding to the skew partition λ/μ , which would contribute $x_1^2 x_2 x_3$ to the skew Schur polynomial.



$$\tag{181}$$

From the strong increase of integers along the rows of a (skew) SSYT, it follows that,

$$s_{\lambda/\mu}(x_1, \dots, x_n) = 0 \quad \text{unless} \quad 0 \leq \lambda_i^t - \mu_i^t \leq n \quad \text{for all} \quad i \geq 1. \quad (182)$$

Note that an example of (182) is given by the fact that $e_k(x_1, \dots, x_N) = s_{(1^k)}(x_1, \dots, x_N) = 0$ for $k > N$.

We have the following expressions for skew Schur polynomials,

$$s_{\lambda/\mu} = \sum_{\nu} c_{\mu\nu}^{\lambda} s_{\nu}, \quad (183)$$

and products of non-skew Schur polynomials,

$$s_{\lambda} s_{\mu} = \sum_{\nu} c_{\lambda\mu}^{\nu} s_{\nu}. \quad (184)$$

The expansion coefficients $c_{\mu\nu}^{\lambda}$ are known as *Littlewood-Richardson coefficients*, which are given by the number of Littlewood-Richardson tableaux of shape ν/λ and weight μ . A Littlewood-Richardson tableau is an SSYT such that, when we read its entries from right to left and top to bottom, any positive integer j appears at least as many times as $j + 1$. Note from (184) that $c_{\mu\nu}^{\lambda} = c_{\nu\mu}^{\lambda}$. For example, of the SSYT's pictured below, the one on the left is a Littlewood-Richardson tableau while the one on the right is not.

$$\begin{array}{c}
 \begin{array}{ccc}
 & & \boxed{1} \boxed{1} \\
 & \boxed{2} & \boxed{2} \\
 \boxed{1} & \boxed{3} &
 \end{array}
 \qquad
 \begin{array}{ccc}
 & & \boxed{1} \boxed{2} \\
 & \boxed{2} & \boxed{2} \\
 \boxed{1} & \boxed{3} &
 \end{array}
 \end{array} \quad (185)$$

We apply the Littlewood-Richardson rule to the special case where one of the diagrams consists of a single row. The result is known as the Pieri formula [50],

$$s_{\lambda} h_n = \sum_{\nu} s_{\nu}, \quad (186)$$

where the sum is over all ν such that ν/λ is a horizontal strip, i.e. a skew diagram with at most one cell in each column. Applying the involution which transposes all diagrams, and therefore exchanges $h_n = s_{(n)}$ with $e_n = s_{(1^n)}$, we have

$$s_{\lambda} e_n = \sum_{\nu} s_{\nu}, \quad (187)$$

where the sum is now over all ν such that ν/λ is a vertical strip, i.e. a skew diagram with at most one cell in each row. The Pieri formula states that $c_{\lambda\mu}^{\nu}$ for $\mu = (n)$ is equal to 1 when ν/λ is a horizontal strip, and zero otherwise. Applying this to $s_{\lambda/(n)}$, we have

$$s_{\lambda/(n)} = \sum_{\nu} s_{\nu}, \quad (188)$$

where the sum is now over all ν such that λ/ν is a horizontal strip. From (187), we also have

$$s_{\lambda/(1^n)} = \sum_{\nu} s_{\nu} , \quad (189)$$

where λ/ν is a vertical strip. The Pieri formula in (188) is illustrated below for $\lambda = (2, 1)$ and $n = 2$, with the cells that are added onto λ are indicated in gray. It is clear that ν/λ is a horizontal strip for all diagrams ν on the right hand side, as there are no two gray cells in any column. For equation (187), one should simply transpose the diagrams.

$$(190)$$

We can use the Pieri rule to demonstrate $\sum_{r=0}^n (-1)^r h_{n-r} e_r = 0$, equation (162). In particular, for $a, b \geq 1$, we have

$$h_a e_b = s_{(a, 1^b)} + s_{(a+1, 1^{b-1})} . \quad (191)$$

The example for $a = 4$ and $b = 3$ gives the following.

$$(192)$$

Plugging this in gives

$$\sum_{r=0}^n (-1)^r h_{n-r} e_r = h_n + (-1)^n e_n + \sum_{r=1}^{n-1} (-1)^r (s_{(n-r, 1^r)} + s_{(n-r+1, 1^{r-1})}) = 0 . \quad (193)$$

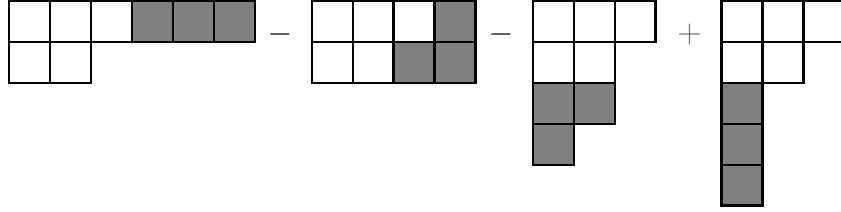
For $1 \leq r \leq n-1$, the summand on the left for any r is cancelled with terms coming from $r-1$ and $r+1$. For $r=0$ and $r=n$, we get the contributions h_n and $(-1)^n e_n$ which cancel with term from $r=1$ and $r=n-1$, respectively. For example, for $n=3$, applying the Pieri formula gives the diagrams below.

$$(194)$$

Further, we have [e.g. theorem 7.17.1, [44]]

$$s_\lambda p_n = \sum_{\nu} (-1)^{\text{ht}(\nu/\lambda)} s_\nu, \quad (195)$$

where ν/λ is a border strip of size n , i.e. a border strip containing n cells. The height $\text{ht}(\nu/\lambda)$ equals the numbers of rows that the border strip occupies minus one. We will also denote these border strips by (e.g.) η with $|\eta| = n$ and write $\nu \setminus \eta$ for the partition obtained from ν after removing the border strip η . For $\lambda = (3, 2)$ and $n = 3$, equation (195) is as follows.



$$(196)$$

Similar to the Pieri formula, equation (195) can be inverted to give the following expression for skew Schur polynomials,

$$\sum_{r=0}^{n-1} (-1)^r s_{\lambda/(n-r, 1^r)} = \sum_{\nu} (-1)^{\text{ht}(\lambda/\nu)} s_\nu, \quad (197)$$

where the sum is now over all ν such that λ/ν is a border strip of size n .

Schur polynomials can be expressed in determinantal form. First of all, the (antisymmetric) Vandermonde determinant can be expressed as

$$\det \left(x_j^{(N-k)} \right)_{j,k=1}^N = \prod_{1 \leq j < k \leq N} (x_j - x_k). \quad (198)$$

We then have

$$s_\lambda(x_j) = \frac{\det \left(x_j^{N-k+\lambda_k} \right)_{j,k=1}^N}{\det \left(x_j^{N-k} \right)_{j,k=1}^N}. \quad (199)$$

(Skew) Schur polynomials can be expressed in terms of elementary symmetric polynomials or complete homogeneous symmetric polynomials via the following determinantal expressions, known as the Jacobi-Trudi identities,

$$\begin{aligned} s_{(\mu/\lambda)} &= \det(h_{\mu_j - \lambda_k - j + k})_{j,k=1}^{\ell(\mu)} = \det(e_{\mu_j^t - \lambda_k^t - j + k})_{j,k=1}^{\mu_1^1}, \\ s_{(\mu/\lambda)^t} &= \det(e_{\mu_j - \lambda_k - j + k})_{j,k=1}^{\ell(\mu)} = \det(h_{\mu_j^t - \lambda_k^t - j + k})_{j,k=1}^{\mu_1^1}. \end{aligned} \quad (200)$$

Again, we see that the expressions in terms of h_j and e_j are related by transposition of the skew diagram,

$(\mu/\lambda) \rightarrow (\mu/\lambda)^t$.

Schur polynomials can also be expanded in terms of power sum polynomials,

$$s_\lambda = \sum_{\alpha} \frac{\chi_{\alpha}^{\lambda}}{z_{\alpha}} p_{\alpha} , \quad (201)$$

where the sum is over all partitions α , z_{α} is defined in (165), and where χ_{α}^{λ} is the character of the symmetric group S_n with $n = |\lambda|$ of an irreducible representation λ associated to a permutation of cycle type α , see e.g. [50], [44]. In fact, α can generally be a weak composition, and χ_{α}^{λ} does not depend on the order of the entries of α . However, in (201), we only sum over a single α corresponding to each cycle type, which is equivalent to summing over partitions. Equation (201) generalizes to the case of a skew partition λ/μ instead of λ . The inverse of (201) is given by

$$p_{\alpha} = \sum_{\lambda} \chi_{\alpha}^{\lambda} s_{\lambda} . \quad (202)$$

It is clear that p_{α} does not depend on the order of the entries of α , it then follows from the above expression that the same is true for χ_{α}^{λ} . To construct the latter objects, we first define a *border-strip tableau* (BST) of shape λ and type α as follows. We take a diagram λ and inscribe it with positive integers such that

1. The integers are weakly increasing along both rows and columns
2. The cells of λ that are inscribed by j form a border strip of size α_j

The resulting object is called a *border strip tableau*, which we denote as $T \in \text{BST}(\lambda, \alpha)$. We show an example below for $\lambda = (7, 5^2, 3, 1)$ and $\alpha = (4^2, 5, 3, 5)$ (remember that α is a composition and its entries are not generally in non-decreasing order) where cells belonging to a single border strip share the same color.

1	1	1	2	2	2	2
1	3	3	3	5		
3	3	5	5	5		
4	4	5				
4						

(203)

Denoting the border strips of length α_j that appear in T as B_j , the height of T is defined as

$$\text{ht}(T) = \sum_{j=1}^{\ell(\alpha)} \text{ht}(B_j) . \quad (204)$$

For example, for the above BST for $\lambda = (7, 5^2, 3, 1)$ and $\alpha = (4^2, 5, 3, 5)$, we have

$$\text{ht}(T) = 1 + 0 + 1 + 1 + 2 = 5 . \quad (205)$$

We then have

$$\chi_\alpha^\lambda = \sum_{T \in \text{BST}(\lambda, \alpha)} (-1)^{\text{ht}(T)} . \quad (206)$$

This is known as the Murnaghan-Nakayama rule, see e.g. [50] or [44]. The Murnaghan-Nakayama rule generalizes to skew diagrams λ/μ .

Consider a simple example we have encountered before. From (202), we have

$$p_n = \sum_\lambda \chi_\lambda^{(n)} s_\lambda = \sum_{r=0}^{n-1} (-1)^r s_{(n-r, 1^r)} . \quad (207)$$

This arises simply from the fact that any Young diagram consisting of a single border strip is a hook shape, as this is the only type of non-skew diagram that has no two by two subdiagram. This gives a sum over all hook shapes containing n cells, $(n-r, 1^r)$, where the sign appears from the fact that $\text{ht}((n-r, 1^r)) = r$. We thus see how equation (175) arises as a special case of (202). To calculate χ_α^λ , one can use the following recursive formula [e.g.(2.4.4) [42]]

$$\chi_\alpha^\lambda = \sum_\rho (-1)^{\text{ht}(\rho)} \chi_{\alpha - \alpha_1}^{\lambda \setminus \rho} , \quad (208)$$

where the sum runs over all border strips ρ of λ containing α_1 cells, $\lambda \setminus \rho$ is the results of removing ρ from λ , and $\alpha - \alpha_j = (\alpha_1, \alpha_2, \dots, \alpha_{j-1}, \alpha_{j+1}, \dots)$. We emphasize again that χ_α^λ does not depend on the order of the entries of α . This implies that we can consecutively apply equation (208) by removing border strips of different sizes in different orders, and end up with the same result. This may at first sight be surprising, as removing border strips in different orders generally leads to a different set of diagrams. Let us consider a simple example, where we remove border strips of sizes 1 and 2 from $\lambda = (3, 2) = \begin{array}{|c|c|c|} \hline \square & \square & \square \\ \hline \square & & \square \\ \hline \end{array}$ in the two different orders. This is indicated in the figure below, where two diagrams connected by an arrow as

$$\lambda \xrightarrow{p_j} \mu \quad (209)$$

indicates that partitions λ and μ are related by the removal of a border strip of size j .

It is clear from figure 2 that going first along p_2 and then along p_1 only leads to the result $\begin{array}{|c|c|} \hline \square & \square \\ \hline \end{array}$, where going first along p_1 and then p_2 leads to $\begin{array}{|c|c|} \hline \square & \square \\ \hline \end{array}$ as well as $\begin{array}{|c|} \hline \square \\ \hline \end{array}$, the latter in two different ways. As indicated in the figure, the dashed line connecting $\begin{array}{|c|c|} \hline \square & \square \\ \hline \end{array}$ and $\begin{array}{|c|} \hline \square \\ \hline \end{array}$ involves the removal of a border strip of height equal to 1, whereas other border strips that are removed in figure 2 have height equal to 0. Consider a

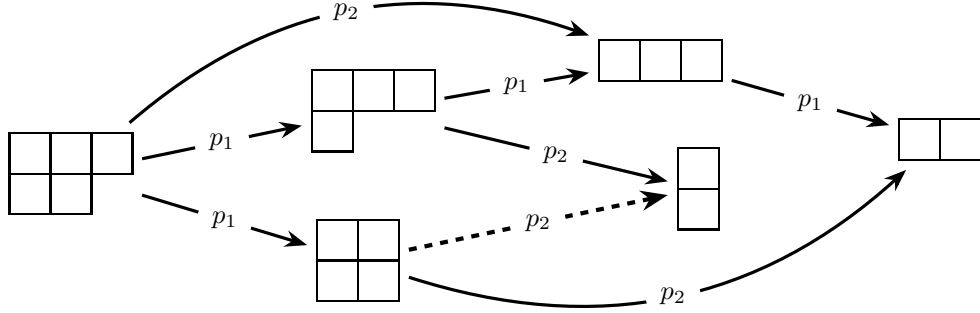


Figure 2: The Young diagram for $\lambda = (3, 2)$ and the removal of border strips of sizes 1 (single cell) and 2 (domino), indicated by p_1 and p_2 , respectively. The dashed line connecting $(2, 2)$ and $(1, 1)$ indicates the only case where a border strip of odd height is removed.

composition α containing at least one row of length one and length two. Applying (208) then gives

$$\begin{aligned} \chi_{\alpha}^{(3,2)} &= \sum_{\mu, \rho} (-1)^{\text{ht}(\rho) + \text{ht}(\mu)} \chi_{\alpha - (2,1)}^{((3,2) \setminus \mu) \setminus \rho} = \chi_{\alpha - (2,1)}^{(2)} + (1 - 1) \chi_{\alpha - (2,1)}^{(1,1)} \\ &= \sum_{\mu, \rho} (-1)^{\text{ht}(\rho) + \text{ht}(\mu)} \chi_{\alpha - (2,1)}^{((3,2) \setminus \rho) \setminus \mu} = \chi_{\alpha - (2,1)}^{(2)} \end{aligned} \quad (210)$$

where μ and ρ are BS of sizes 1 and 2, respectively, and where $\alpha - (2, 1)$ indicates that we remove a row of length 1 and a row of length 2 from α . Note the different order of removal of μ and ρ in the top and bottom rows. We see that the sign given by $(-1)^{\text{ht}(\rho)}$ ensures that removing border strips of different sizes in different orders, as it leads to the cancellation between various ways to arrive at certain diagrams that are unattainable via a different order of removal. We treat the removal of border strips from $\lambda = \begin{array}{|c|c|c|} \hline \square & \square & \square \\ \hline \square & \square & \square \\ \hline \end{array}$ more extensively in section 2.3, see figure 1.

Let us consider the object $(p_n)^k$. Using (202), we have

$$(p_n)^k = \sum_{\lambda} \chi_{(n^k)}^{\lambda} s_{\lambda} . \quad (211)$$

From (206) (or (195) with $\lambda = \emptyset$), the $\chi_{(n^k)}^{\lambda}$ appearing in (211) are of the following form

$$\chi_{(n^k)}^{\lambda} = \sum_{T \in \text{BST}(\lambda, (n^k))} (-1)^{\text{ht}(T)} , \quad (212)$$

where the sum is over all *border strip tableaux* of shape λ and type $\alpha = (n^k)$. For $\alpha = (n^k)$, it has been shown that the expansion in (212) is cancellation-free [corollary 10, [41]]. That is, for any fixed choice of λ , all BST's appear with the same sign, so that

$$\chi_{(n^k)}^{\lambda} = \pm \sum_{T \in \text{BST}(\lambda, (n^k))} 1 . \quad (213)$$

In fact, there is a more general result [theorem 2.7.27 in [42]], which states that

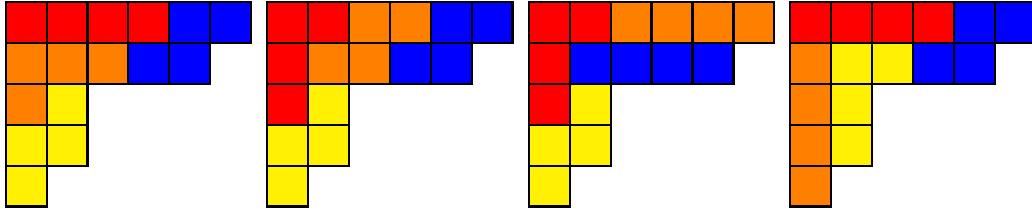
$$\chi_{(n^k)}^{\lambda/\mu} = \pm \sum_{T \in \text{BST}(\lambda/\mu, (n^k))} 1. \quad (214)$$

In the above expression, μ is the so-called n -core of λ , which is the diagram that remains after removing the maximum possible of border strips of size n . We denote by $w(\lambda)$ the n -weight of λ , which is the number of border strips of size n which one has to remove to obtain the n -core of λ . The number of partitions with n -core given by μ is then given by [theorem 2.7.17 in [42]]

$$b(w) = \sum_{\{w_j\}} \prod_{j=1}^n p(w_j), \quad (215)$$

where the sum is over all sets of n non-negative integers w_j satisfying $\sum_{j=1}^n w_j = w(\lambda)$, and where $p(w_j)$ is the number of partitions of w_j .

We illustrate (214) for λ with empty n -core (i.e. (213)), in particular, for $\lambda = (6, 5, 2^2, 1)$ and $\alpha = (n^k) = (4^4)$. This gives the following border strip tableaux, where border strips again share the same color.


(216)

We see that the heights of the tableaux are given, from left to right, by 4, 6, 4, 6, so that $(-1)^{\text{ht}(T)} = 1$. Note that the two leftmost BST's appear with multiplicity two, as one can remove the yellow and blue border strips in either order. This means that $\chi_{(4^4)}^{(6,5,2^2,1)} = 6$. We see, then, that all BST's contribute with the same sign as they are all of even height. Equation (213) states that the BST's *always* appear with the same sign for any choice of λ and (n^k) . One can see that this generalizes to skew partitions λ/ρ by considering λ and ρ for which $\text{BST}(\lambda, (n^k))$ and $\text{BST}(\rho, (n^k))$ are non-empty, and using the fact that $\text{ht}(T_{\lambda/\rho}) = \text{ht}(T_\lambda) - \text{ht}(T_\rho)$, where $T_{\lambda/\rho}$ is a border strip tableau of type (n^k) for some k .

B Correlation functions of long-range random walks

We summarize here the derivation which relates correlation functions of one-dimensional LRRW models to weighted integrals over $U(N)$ with insertion of Schur polynomials, following [25], [26], and [27]. We first consider the XX0-model, that is, the XX-model with zero magnetic field,

$$\hat{H} = \sum_{m,n} \Delta_{n,m} \sigma_n^- \sigma_m^+ \quad , \quad \Delta_{m,n} = \delta_{n+1,m} + \delta_{n-1,m} . \quad (217)$$

We start with state with holes at all sites

$$|\uparrow\rangle = \otimes_n |\uparrow\rangle_n = \otimes_n \begin{pmatrix} 1 \\ 0 \end{pmatrix}_n, \quad (218)$$

which satisfies

$$\hat{H} |\uparrow\rangle = 0. \quad (219)$$

Define the correlation function

$$F_{j;l}(\tau) = \langle \uparrow | \sigma_j^+ e^{-\tau \hat{H}} \sigma_l^- | \uparrow \rangle. \quad (220)$$

For now, we consider τ to be a general complex number, but we will mostly be interested in the case where $\tau = it$ where t is a real-valued time parameter. Using

$$[\sigma_n^+, \sigma_m^-] = \sigma_n^z \delta_{m,n}, \quad [\sigma_n^z, \sigma_m^\pm] = \pm 2\sigma_n^\pm \delta_{m,n}, \quad (221)$$

we have

$$[\hat{H}, \sigma_k^-] = \sum_m \Delta_{m,k} \sigma_m^- \sigma_k^z, \quad (222)$$

which we apply to find

$$\frac{d}{d\tau} F_{j;l}(\tau) = - \langle \uparrow | \sigma_j^+ e^{-\tau \hat{H}} \hat{H} \sigma_l^- | \uparrow \rangle = \sum_m \Delta_{l,m} F_{j;m}(\tau). \quad (223)$$

In particular, for the XX0-model, where $\Delta_{m,n} = \delta_{n+1,m} + \delta_{n-1,m}$,

$$\frac{d}{d\tau} F_{j;l}(\tau) = F_{j;l+1}(\tau) + F_{j;l-1}(\tau). \quad (224)$$

We will generally consider the case where $\Delta_{m,n} = \Delta_{m-n} = a_{m-n}$, i.e. the hopping amplitude depends only on the (positive or negative) distance between lattice sites m and n . In this case, $\Delta_{m,n}$ is a Toeplitz matrix, i.e. it is constant along its diagonals. Taking $L + 1$ lattice sites, as in [25], the hamiltonian is generally of the form,

$$\hat{H} = - \sum_{m=0}^L \sum_{n=1}^{(L-1)/2} (a_n \sigma_m^- \sigma_{m+n}^+ + a_{-n} \sigma_m^- \sigma_{m-n}^+) + \frac{\hbar}{2} \sum_{m=0}^L (\sigma_m^z - \mathbf{1}), \quad (225)$$

where we demand that $a_{-k} = a_k^*$, the complex conjugate of a_k . The hopping parameters may acquire a non-zero imaginary component e.g. as the result of gauge flux attachment. We then have

$$[\hat{H}, \sigma_k^-] = - \sum_n (a_n \sigma_{k-n}^- \sigma_n^z + a_{-n} \sigma_{k+n}^- \sigma_k^z) - \hbar \sigma_k^-, \quad (226)$$

so that

$$\frac{d}{d\tau} F_{j;l}(\tau) = \sum_n (a_n F_{j-n;l} + a_{-n} F_{j+n;l}) + h F_{j;l} . \quad (227)$$

It is clear that $F_{j;l}$ only depends on $|j - l|$. The generating function $f(z; \tau) = \sum_{j \in \mathbb{Z}} F_{j;l} z^{j-l}$ is given by [25], [27]

$$f(z; \tau) = \exp \left(\tau \sum_{k \in \mathbb{Z}} a_k z^k \right) , \quad (228)$$

where we set $a_0 = h$. Consider now the multi-particle correlation function, with $N \leq L$,

$$F_{j_1, \dots, j_N; l_1, \dots, l_N}(\tau) = \left\langle \uparrow \left| \sigma_{j_1}^+ \dots \sigma_{j_N}^+ e^{-\tau \hat{H}} \sigma_{l_1}^- \dots \sigma_{l_N}^- \right| \uparrow \right\rangle . \quad (229)$$

We impose periodic boundary conditions for simplicity. However, we will be taking the thermodynamic limit and considering only configurations which contain an infinite sequence of adjacent holes, with the particles either confined to a finite interval in their initial configuration or starting with an infinite sequence of adjacent particles. As such, imposing periodic boundary conditions will have no effect on our final result. We then have,

$$\begin{aligned} \frac{d}{d\tau} F_{j_1, \dots, j_N; l_1, \dots, l_N}(\tau) &= \sum_{k, m} (a_k F_{j_1, \dots, j_N; l_1, \dots, l_m + k, \dots, l_N}(\tau) + a_k F_{j_1, \dots, j_N; l_1, \dots, l_m - k, \dots, l_N}(\tau)) + \\ &+ N h F_{j_1, \dots, j_N; l_1, \dots, l_N}(\tau) . \end{aligned} \quad (230)$$

Remember that the summations over k and m are over different ranges. The solution to equation (230) is of determinantal form [25], [26], [27],

$$F_{j_1, \dots, j_N; l_1, \dots, l_N}(\tau) = \det (F_{j_r; l_s}(\tau))_{r, s=1}^N . \quad (231)$$

From the initial condition $F_{j;l}(0) = \delta_{j,l}$, it follows that,

$$F_{j;l}(\tau) = \frac{1}{L+1} \sum_{s=0}^L \exp \left(\tau \sum_k^{(L-1)/2} a_k e^{ik\theta_s} \right) e^{i(j-l)\theta_s} , \quad \theta_s = \frac{2\pi}{L+1} (s - L/2) . \quad (232)$$

Using the determinantal expression for Schur functions in equation (199), we have

$$\begin{aligned} F_{j_1, \dots, j_N; l_1, \dots, l_N}(\tau) &= \frac{1}{(L+1)^N} \sum_{\{s_j\}} \exp \left(\tau \sum_{j=1}^N \sum_k^{(L-1)/2} a_k e^{ik\theta_{s_j}} \right) \prod_{1 \leq j < k \leq N} |e^{i\theta_{s_j}} - e^{i\theta_{s_k}}|^2 \times \\ &\times s_\lambda(e^{i\theta_{s_1}}, \dots, e^{i\theta_{s_N}}) s_\mu(e^{-i\theta_{s_1}}, \dots, e^{-i\theta_{s_N}}) , \end{aligned} \quad (233)$$

with $\lambda_r = j_r - N + r$ and $\mu_s = l_s - N + s$. We shift j_r and l_r by N , such that

$$\lambda_r = j_r + r \quad , \quad \mu_s = l_s + s \quad . \quad (234)$$

This is merely a convenient relabelling of our lattice sites. We now take $L \rightarrow \infty$. Demanding that the hopping parameters a_k decay at least as $a_k \sim k^{-1-\epsilon}$ for some $\epsilon > 0$, we then have [25], [26], [27],

$$\begin{aligned} F_{j_1, \dots, j_N; l_1, \dots, l_N}(\tau) &= \mathcal{N} e^{Nh\tau} \int_{-\pi}^{\pi} d\theta_1 \dots \int_{-\pi}^{\pi} d\theta_N \prod_{1 \leq r < s \leq N} |e^{i\theta_r} - e^{i\theta_s}|^2 \prod_{k=1}^N f(e^{i\theta_k}; \tau) \times \\ &\times s_{\lambda}(e^{i\theta_1}, \dots, e^{i\theta_N}) s_{\mu}(e^{-i\theta_1}, \dots, e^{-i\theta_N}) \quad , \end{aligned} \quad (235)$$

where the weight function $f(z; \tau)$ is given in (228). We include in equation (235) a normalization factor \mathcal{N} which is determined by demanding

$$F_{j_1, \dots, j_N; l_1, \dots, l_N}(0) = \prod_{k=1}^M \delta_{j_k, l_k} \quad . \quad (236)$$

Note that (235) is the expression for an integral over $U(N)$ weighted by some weight function f with insertion of Schur polynomials s_{λ} and s_{μ} . In particular, writing $s_{\lambda}(U) = s_{\lambda}(e^{i\theta_j})$, where $e^{i\theta_j}$ are the eigenvalues of U , we have

$$F_{j_1, \dots, j_N; l_1, \dots, l_N}(\tau) = \int_{U(N)} dU \det(f(U)) s_{\lambda}(U) s_{\mu}(U^{-1}) \quad . \quad (237)$$

When we take the limit $\tau \rightarrow 0$, we have $f = 1$, which recovers the circular unitary ensemble (CUE) i.e. the integral over the Haar measure on $U(N)$. In this case $s_{\lambda/\mu}(x) = 0$ for any $\lambda/\mu \neq \emptyset$, which greatly simplifies many calculations. If $\lambda = \emptyset = \mu$, we have $j_r = -r = l_r$, and we are simply considering the return probability for N adjacent particles [45], [46], see also [47]. In general, we will write

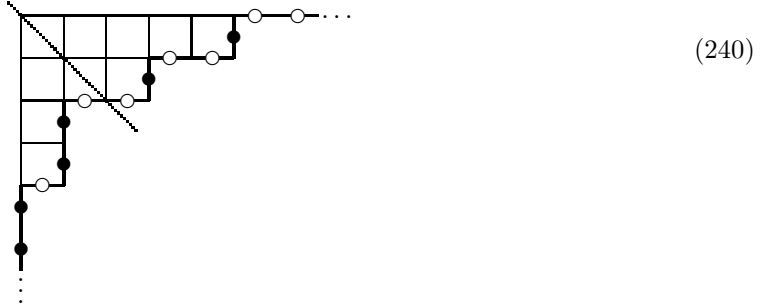
$$F_{\lambda; \mu}(\tau) = F_{j_1, \dots, j_N; l_1, \dots, l_N}(\tau) \quad , \quad (238)$$

where equation (234) expresses the relation between λ , μ and $\{j_r\}$, $\{l_r\}$, respectively. We will write the state corresponding to an empty diagram as $|\emptyset\rangle$. This can be illustrated as follows, where a particle is indicated by a black dot and hole by a white dot and the vertical line separates lattice sites 0 and 1.

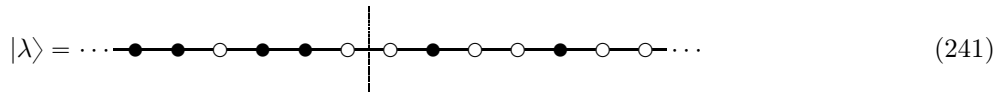
$$|\emptyset\rangle = \cdots \bullet \bullet \bullet \bullet \bullet \left| \begin{array}{c} \bullet \\ \bullet \\ \bullet \\ \bullet \\ \bullet \end{array} \right. \circ \circ \circ \circ \circ \cdots \quad (239)$$

For non-empty λ, μ , the object $F_{\lambda; \mu}$ corresponds to a correlation function where certain particles are shifted by a finite number of sites. The well-known association between Young diagrams and 1D configurations of spins (or fermions, or any other binary variable) is as follows. We place a diagram in the corner where infinitely long horizontal and vertical lines meet. We number the edges of these horizontal and vertical lines, as well as external edges (i.e. those on the lower right) of the diagram, such that the main diagonal

passes between sites 0 and 1. We then associate a particle to all vertical edges and a hole to all horizontal edges. This association is illustrated³ below for $\lambda = (5, 3, 1^2)$, where we add a dotted diagonal line which separates lattice sites 0 and 1.



The configuration corresponding to the above diagram is illustrated below, with again a dotted line separating sites 0 and 1.



It is clear from the above association between diagrams and particle-hole configurations that λ affects particles from position $j = -\ell(\lambda) + 1$ up to $j = \lambda_1$, which means that there is an interval containing $\ell(\lambda)$ particles and λ_1 holes, the leftmost of which is a hole and the rightmost a particle. In particular, the state $|\lambda\rangle$ has a hole at $j = -\ell(\lambda) + 1$ and a particle at $j = \lambda_1$, and the remaining $\ell(\lambda) - 1$ particles and $\lambda_1 - 1$ holes are distributed over sites $j = \{-\ell(\lambda) + 2, -\ell(\lambda) + 3, \dots, \lambda_1 - 1\}$, which can be seen explicitly for $\lambda = (5, 3, 1^2)$ above.

C Evaluating unitary matrix integrals

We briefly review the evaluation of weighted unitary integrals over Schur polynomials. We start from an absolutely integrable function on the unit circle in \mathbb{C} ,

$$f(e^{i\theta}) = \sum_{k \in \mathbb{Z}} d_k e^{ik\theta} . \quad (242)$$

We require that $f(e^{i\theta})$ satisfies the assumptions of Szegő's theorem. That is, we write $f(e^{i\theta})$ as

$$f(e^{i\theta}) = \exp \left(\sum_{k \in \mathbb{Z}} c_k e^{ik\theta} \right) , \quad (243)$$

³We made grateful use of the illustrations in the excellent review [51] by Zinn-Justin, which we adapt here for our purposes.

and demand that

$$\sum_{k \in \mathbb{Z}} |c_k| < \infty \quad , \quad \sum_{k \in \mathbb{Z}} |k| |c_k|^2 < \infty \quad . \quad (244)$$

Writing

$$D_N(f) = \det(T_N(f)) = \det(d_{j-k})_{j,k=1}^N \quad , \quad (245)$$

the strong Szegő limit theorem then states that [52],

$$\lim_{N \rightarrow \infty} \frac{D_N(f)}{e^{-Nc_0}} = \exp \left(\sum_{k=1}^{\infty} k c_k c_{-k} \right) \quad . \quad (246)$$

The above determinant and various generalization thereof can be related to integrals over the group of N by N unitary matrices with some weight function f with the insertion of Schur polynomials. Take the following matrix,

$$T_N^{\lambda, \mu}(f) = (d_{j-\lambda_j-k+\mu_k})_{j,k=1}^N \quad . \quad (247)$$

Then [53], [54],

$$\begin{aligned} D_N^{\lambda, \mu}(f) &:= \det T_N^{\lambda, \mu}(f) = \int_{U(N)} s_{\lambda}(U^{-1}) s_{\mu}(U) \det f(U) dU \\ &= \frac{1}{N!(2\pi)^N} \int_0^{2\pi} s_{\lambda}(e^{-i\theta_1}, \dots, e^{-i\theta_M}) s_{\mu}(e^{i\theta_1}, \dots, e^{i\theta_M}) \prod_{j=1}^M f(e^{i\theta_j}) \prod_{1 \leq j < k \leq N} |e^{i\theta_j} - e^{i\theta_k}|^2 d\theta_j \\ &= \det (d_{j-\lambda_j-k+\mu_k})_{j,k=1}^N \quad . \end{aligned} \quad (248)$$

From the above expression, one can see that $D_N^{\lambda, \mu}(f)$ can be expressed as a minor of $T_{N+k}(f)$, where $k = \max\{\lambda_1, \mu_1\}$. We remind the reader that a minor of some matrix M is the determinant of a matrix obtained from M by removing some of its rows and columns. In our case, the rows and columns which are removed are specified by λ and μ . We write the expectation value $\langle \dots \rangle$ with respect to the matrix model with weight function f as

$$\langle s_{\lambda}(U) s_{\mu}(U^{-1}) \rangle = \frac{\int s_{\lambda}(U) s_{\mu}(U^{-1}) \det f(U) dU}{\int \det f(U) dU} \quad . \quad (249)$$

We will often neglect to write $U^{\pm 1}$ explicitly, instead writing $\langle s_{\lambda} s_{\mu} \rangle$ or, more generally, $\langle AB \rangle$ for symmetric polynomials A and B . For two functions of the form

$$a(z) = \sum_{k \leq 0} a_k z^k \quad , \quad b(z) = \sum_{k \geq 0} b_k z^k \quad , \quad (250)$$

the associated Toeplitz matrix satisfies

$$T(ab) = T(a)T(b) . \quad (251)$$

Let us therefore write $f(e^{i\theta})$ as follows

$$f(z) = H(x; z)H(y; z^{-1}) , \quad (252)$$

where $H(x; z)$ is the generating function of the homogeneous symmetric polynomials h_k given in (161) and where we assume that $h_k(x)$ and $h_k(y)$ are square-summable, i.e. $\sum_k |h_k|^2 < \infty$. We can also define our weight function as

$$f(z) = E(x; z)E(y; z^{-1}) , \quad (253)$$

at the cost replacing h_j by e_j everywhere, which is equivalent to transposing all diagrams. We repeat that the CUE corresponds to $f = 1$, which corresponds to $x_j = 0$ for all j for both $f(z) = H(x; z)H(y; z^{-1})$ and $f(z) = E(x; z)E(y; z^{-1})$. We will consider the case where $f(z) = H(x; z)H(y; z^{-1})$ unless stated otherwise.

It was shown by Gessel [55] that $D_N(f)$ can be expressed in terms of Schur polynomials as

$$D_N(f) = \sum_{\ell(\nu) \leq N} s_\nu(x)s_\nu(y) . \quad (254)$$

Equation (248) can be similarly expressed in terms of (skew) Schur polynomials [53], [56], [57],

$$\int s_\lambda(U)s_\mu(U^{-1}) \det f(U) dU = \sum_{\ell(\rho) \leq N} s_{\rho/\lambda}(x)s_{\rho/\mu}(y) . \quad (255)$$

We now take the limit $N \rightarrow \infty$. From (255) and the fact that [Chapter I.5, example 26 in [50]]

$$\sum_{\rho} s_{\rho/\lambda}(x)s_{\rho/\mu}(y) = \sum_{\nu} s_{\mu/\nu}(x)s_{\lambda/\nu}(y) \sum_{\eta} s_{\eta}(x)s_{\eta}(y) , \quad (256)$$

where the sums run over all partitions, it follows that [56], [57]

$$\langle s_\lambda(U)s_\mu(U^{-1}) \rangle = \sum_{\nu} s_{\lambda/\nu}(y)s_{\mu/\nu}(x) , \quad (257)$$

where the sum runs over all ν such that $\nu \subseteq \lambda, \mu$. As noted at equation (253), we can also define $f(z) = E(x; z)E(y; z^{-1})$ at the cost of transposing all diagrams. In this case, one has

$$\langle s_\lambda(U)s_\mu(U^{-1}) \rangle = \sum_{\nu} s_{(\lambda/\nu)^t}(y)s_{(\mu/\nu)^t}(x) , \quad (258)$$

We will consider $f(z) = H(x; z)H(y; z^{-1})$ and apply (257) unless stated otherwise. If we take $\mu = \emptyset$ in

(257), the only choice for ν that contributes to the above sum is $\nu = \emptyset$ as well, and we have

$$\langle s_\lambda(U) \rangle = s_\lambda(y) \quad , \quad \langle s_\mu(U^{-1}) \rangle = s_\mu(x) \quad . \quad (259)$$

We also define the connected expectation value ,

$$\langle s_\lambda(U)s_\mu(U^{-1}) \rangle_c := \langle s_\lambda(U)s_\mu(U^{-1}) \rangle - \langle s_\lambda(U) \rangle \langle s_\mu(U^{-1}) \rangle \quad , \quad (260)$$

which corresponds to subtracting the contribution corresponding to $\nu = \emptyset$ in (257).

6 References

- [1] P. Ginsparg and G. Moore. Lectures on 2d gravity and 2d string theory (tasi 1992). arXiv:9304011, 1993.
- [2] P. Di Francesco, P. Ginsparg, and J. Zinn-Justin. 2d gravity and random matrices. *Physics Reports*, 254(1-2):1–133, 1995.
- [3] P.J. Forrester. *Log-Gases and Random Matrices*. London Mathematical Society Monographs. Princeton University Press, Princeton, NJ, 2010.
- [4] B. Eynard, T. Kimura, and S. Ribault. Random matrices. arXiv:1510.04430, 2015.
- [5] M.E. Fisher. Walks, walls, wetting, and melting. *Journal of Statistical Physics*, 34:667–729, 1984.
- [6] P. J. Forrester. Vicious random walkers in the limit of a large number of walkers. *Journal of Statistical Physics*, 56(5-6):767–782, 1989.
- [7] P.J. Forrester. Exact solution of the lock step model of vicious walkers. *Journal of Physics A: Mathematical and General*, 23(7):1259–1273, 1990.
- [8] A.J. Guttmann, A.L. Owczarek, and X.G. Viennot. Vicious walkers and Young tableaux i: without walls. *Journal of Physics A: Mathematical and General*, 31(40):8123–8135, 1998.
- [9] J. Baik. Random vicious walks and random matrices. *Communications on Pure and Applied Mathematics*, 53:1385–1410, 2000.
- [10] C. Krattenthaler, A.J. Guttmann, and X.G. Viennot. Vicious walkers, friendly walkers and Young tableaux: II. with a wall. *Journal of Physics A: Mathematical and General*, 33(48):8835–8866, 2000.
- [11] T. Nagao and P.J. Forrester. Vicious random walkers and a discretization of gaussian random matrix ensembles. *Nuclear Physics B*, 620(3):551–565, 2002.
- [12] M. Katori and H. Tanemura. Scaling limit of vicious walks and two-matrix model. *Physical Review E*, 66(1), 2002.
- [13] Andrei Okounkov. The uses of random partitions, 2003.

- [14] M. Jimbo and T. Miwa. Solitons and Infinite Dimensional Lie Algebras. *Publ. Res. Inst. Math. Sci. Kyoto*, 19:943, 1983.
- [15] A.Yu. Morozov. Integrability and matrix models. *Physics-Uspeski*, 37(1):1–55, 1994.
- [16] A. Yu. Orlov. Tau functions and matrix integrals. math-ph/0210012, 2002.
- [17] E. Bettelheim, A. Abanov, and P. Wiegmann. Nonlinear dynamics of quantum systems and soliton theory. *Journal of Physics A: Mathematical and Theoretical*, 40:F193, 2007.
- [18] J. Harnad and A.Yu. Orlov. Fermionic construction of partition functions for two-matrix models and perturbative schur function expansions. *Journal of Physics A: Mathematical and General*, 39(28):8783–8809, 2006.
- [19] J. Harnad and A. Yu. Orlov. Polynomial KP and BKP tau-functions and correlators. *Annales Henri Poincaré*, 22(9):3025–3049, 2021.
- [20] A. Morozov. Matrix models as integrable systems, 1995.
- [21] A. Mironov and A. Morozov. On the complete perturbative solution of one-matrix models. *Physics Letters B*, 771:503–507, aug 2017.
- [22] A. Mironov, A. Morozov, and Z. Zakirova. New insights into superintegrability from unitary matrix models. *Physics Letters B*, 831:137178, aug 2022.
- [23] Ofer Aharony, Joseph Marsano, Shiraz Minwalla, Kyriakos Papadodimas, and Mark Van Raamsdonk. The deconfinement and hagedorn phase transitions in weakly coupled large n gauge theories. *Comptes Rendus Physique*, 5(9-10):945–954, nov 2004.
- [24] S. Murthy. Unitary matrix models, free fermion ensembles, and the giant graviton expansion. arXiv:2202.06897, 2022.
- [25] N.M. Bogoliubov. XX0 heisenberg chain and random walks. *Journal of Mathematical Sciences*, 138:5636–5643, 2006.
- [26] N.M. Bogoliubov, A.G. Pronko, and J. Timonen. Scaling of many-particle correlations in a dissipative sandpile, 2011.
- [27] D. Pérez-García and M. Tierz. Chern–Simons theory encoded on a spin chain. *J. Stat. Mech.*, 1601(1):013103, 2016.
- [28] E.A. Yuzbashyan and B.L. Altshuler. Migdal-Eliashberg theory as a classical spin chain. *Phys. Rev. B*, 106:014512, 2022.
- [29] X. Deng, V.E. Kravtsov, G.V. Shlyapnikov, and L. Santos. Duality in power-law localization in disordered one-dimensional systems. *Physical Review Letters*, 120(11), 2018.
- [30] P.A. Nosov, I.M. Khaymovich, and V.E. Kravtsov. Correlation-induced localization. *Physical Review B*, 99(10), 2019.

- [31] N. Defenu, T. Donner, T. Macrì, G. Pagano, S. Ruffo, and A. Trombettoni. Long-range interacting quantum systems. *arXiv:2109.01063*, 2021.
- [32] L. Santilli and M. Tierz. Phase transition in complex-time Loschmidt echo of short and long range spin chain. *Journal of Statistical Mechanics: Theory and Experiment*, 2020(6):063102, 2020.
- [33] C. Malyshev and N.M. Bogoliubov. Heisenberg XX chain, non-homogeneously parameterised generating exponential, and diagonally restricted plane partitions. *arxiv.2011.05148*, 2020.
- [34] David Pérez-García, Leonardo Santilli, and Miguel Tierz. Dynamical quantum phase transitions from random matrix theory, 2022.
- [35] T. Gorin, T. Prosen, T.H. Seligman, and M. Žnidarič. Dynamics of Loschmidt echoes and fidelity decay. *Physics Reports*, 435(2-5):33–156, 2006.
- [36] M. Gärttner, J.G. Bohnet, A. Safavi-Naini, M.L. Wall, J.J. Bollinger, and A.M. Rey. Measuring out-of-time-order correlations and multiple quantum spectra in a trapped-ion quantum magnet. *Nature Physics*, 13(8):781–786, 2017.
- [37] J. Braumüller, A.H. Karamlou, Y. Yanay, B. Kannan, D. Kim, M. Kjaergaard, A. Melville, B.M. Niedzielski, Y. Sung, A. Vepsäläinen, R. Winik, J.L. Yoder, T.P. Orlando, S. Gustavsson, C. Tahan, and W.D. Oliver. Probing quantum information propagation with out-of-time-ordered correlators. *Nature Physics*, 18(2):172–178, 2021.
- [38] S. K. Zhao, Zi-Yong Ge, Zhongcheng Xiang, G. M. Xue, H. S. Yan, Z. T. Wang, Zhan Wang, H. K. Xu, F. F. Su, Z. H. Yang, He Zhang, Yu-Ran Zhang, Xue-Yi Guo, Kai Xu, Ye Tian, H. F. Yu, D. N. Zheng, Heng Fan, and S. P. Zhao. Probing operator spreading via floquet engineering in a superconducting circuit, 2021.
- [39] P. Diaconis and M. Shahshahani. On the eigenvalues of random matrices. *Journal of Applied Probability*, 31(A):49–62, 1994.
- [40] W.L. Vleeshouwers and V. Gritsev. Topological field theory approach to intermediate statistics. *SciPost Phys.*, 10:146, 2021.
- [41] D.E. White. A bijection proving orthogonality of the characters of sn . *Advances in Mathematics*, 50(2):160–186, 1983.
- [42] G. James and A. Kerber. *The Representation Theory of the Symmetric Group*. Encyclopedia of Mathematics and its Applications. Cambridge University Press, 1984.
- [43] P. Diaconis and S. Evans. Linear functionals of eigenvalues of random matrices. *Transactions of the American Mathematical Society*, 353, 2000.
- [44] R.P. Stanley and S. Fomin. *Enumerative Combinatorics: Volume 2*. Cambridge Studies in Advanced Mathematics. Cambridge University Press, 1999.

- [45] J. Viti, J.M. Stéphan, J. Dubail, and M. Haque. Inhomogeneous quenches in a fermionic chain: exact results. *EPL (Europhysics Letters)*, 115, 2015.
- [46] L. Wei, R. Pitaval, and O. Tirkkonen J. Corander. From random matrix theory to coding theory: Volume of a metric ball in unitary group. *IEEE Transactions on Information Theory*, PP, 2015.
- [47] P.L. Krapivsky, J.M. Luck, and K. Mallick. Quantum return probability of a system of n non-interacting lattice fermions. *Journal of Statistical Mechanics: Theory and Experiment*, 2018(2):023104, 2018.
- [48] E. Bogomolny. Spectral statistics of random toeplitz matrices. *Physical Review E*, 102(4):040101, 2020.
- [49] E. Bogomolny and O. Giraud. Statistical properties of structured random matrices. *Physical Review E*, 103(4):042213, 2021.
- [50] I.G. Macdonald. *Symmetric Functions and Hall Polynomials*. Oxford classic texts in the physical sciences. Clarendon Press, 1998.
- [51] P. Zinn-Justin. Six-vertex, loop and tiling models: integrability and combinatorics. arXiv:0901.0665, 2009.
- [52] G. Szegő. Ein Grenzwertsatz über die Toeplitzischen Determinanten einer reellen positiven Funktion. *Math. Ann.*, 76:490–503, 1915.
- [53] D. Bump and P. Diaconis. Toeplitz minors. *Journal of Combinatorial Theory, Series A*, 97(2):252 – 271, 2002.
- [54] M. Adler and P. van Moerbeke. Virasoro action on schur function expansions, skew Young tableaux, and random walks. *Communications on Pure and Applied Mathematics*, 58:362–408, 2003.
- [55] I.M. Gessel. Symmetric functions and p-recursiveness. *Journal of Combinatorial Theory, Series A*, 53(2):257 – 285, 1990.
- [56] D. García-García and M. Tierz. Toeplitz minors and specializations of skew schur polynomials. *Journal of Combinatorial Theory, Series A*, 172:105201, 2020.
- [57] D. García-García and M. Tierz. Matrix models for classical groups and toeplitz \pm hankel minors with applications to chern–simons theory and fermionic models. *Journal of Physics A: Mathematical and Theoretical*, 53(34):345201, 2020.